scientific reports

Check for updates

OPEN

Improving maize yield and drought tolerance in field conditions through activated biochar application

Muhammad Bilal Naeem[1], Summera Jahan[1,2]✉, Audil Rashid[1], Anis Ali Shah[3]✉, Vaseem Raja[4] & Mohamed A. El-Sheikh[5]

Amidst depleting water resources, rising crop water needs, changing climates, and soil fertility decline from inorganic modifications of soil, the need for sustainable agricultural solutions has been more pressing. The experimental work aimed to inspect the potential of organically activated biochar in improving soil physicochemical and nutrient status as well as improving biochemical and physiological processes, and optimizing yield-related attributes under optimal and deficit irrigation conditions. Biochar enhances soil structure, water retention, and nutrient availability, while improving plant nutrient uptake and drought resilience. The field experiment with maize crop was conducted in Hardaas Pur (32°38.37′N, 74°9.00′E), Gujrat, Pakistan. The experiment involved the use of DK-9108, DK-6321, and Sarhaab maize hybrid seeds, with five moisture levels of evapotranspiration (100% ETC, 80% ETC, 70% ETC, 60% ETC, and 50% ETC) maintained throughout the crop seasons. Furthermore, activated biochar was applied at three levels: 0 tons/ha (no biochar), 5 tons per hectare, and 10 tons per hectare. The study's findings revealed significant improvements in soil organic matter, bulk density, nutrient profile and total porosity with biochar supplementation in soil. Maize plants grown under lower levels of ETC in biochar supplemented soil had enhanced membrane stability index (1.6 times higher) increased protein content (1.4 times higher), reduced malondialdehyde levels (0.7 times lower), improved antioxidant enzyme activity (1.3 times more SOD and POD activity, and 1.2 times more CAT activity), improved relative growth (1.05 times more) and enhanced yield parameters (26% more grain and stover yield, 16% more 1000-seed weight, 29% more total seed weight, 33% more apparent water productivity) than control. Additionally, among the two biochar application levels tested, the 5 tons/ha dose demonstrated superior efficiency compared to the 10 tons/ha biochar dose.

Keywords Soil health, Drought tolerance, Water use efficiency, Crop evapotranspiration, Penman-Monteith equation

Global environmental challenges are intensifying due to urbanization, altering climatic patterns, and exponential population growth; Pakistan is particularly vulnerable to the repercussions of these developments[1,2]. Water scarcity is one of the consequences of these unusual weather patterns, mostly brought on by the increase in temperature. This has a direct impact on quality and quantity of agricultural productivity[3]. Drought conditions have become increasingly prevalent worldwide over the last century[4]. Numerous regions in Pakistan have been confronted with drought conditions ranging from moderate to severe[5]. The Pakistan Council of Research in Water Resources (PCRWR) predicts Pakistan will experience its worst water shortage by 2025[6]. Because of rising crop water demand and decreasing water supply, ensuring a sufficient food supply becomes an enormous challenge in the long run[7]. Elevated levels of CO_2 and temperature stimulate increased evapotranspiration; consequently, plants demand a greater quantity of water to meet their fundamental growth requirements[8]. Moreover, rising food demand can be met by overharvesting, but this can lead to soil deterioration and soil infertility if harvesting and crop sowing are not managed appropriately[9]. A variety of soil amendments, including manure, organic

[1]Department of Botany, Hafiz Hayat Campus, University of Gujrat, Gujrat, Pakistan. [2]Institute of Botany, University of the Punjab, Lahore, Pakistan. [3]Department of Botany, Division of Science and Technology, University of Education, Lahore, Pakistan. [4]University Centre for Research and Development, Chandigarh University, Gharuan, Mohali, Punjab 140413, India. [5]Botany and Microbiology Department, College of Science, King Saud University, Riyadh, Saudi Arabia. ✉email: Summera.botany@pu.edu.pk; anisalibot@gmail.com

matter, lime, and gypsum, are utilised for the purpose of enhancing soil fertility[10]. However, integrating biochar into the soil is the most efficient and environmentally beneficial method for preserving soil fertility[11]. The biochar is generated through the process of pyrolysis of organic waste underneath anaerobic conditions and the resultant solid product with a highly recalcitrant carbon proportion is called biochar[12]. Biochar has many potential benefits as a soil amendment it improves soil structure, decreases bulk density of soil, and neutralizes acidic soil[13]. It also improves pore volume and soil porosity, enhances soil cation exchange capacity[14], and facilitates a positive change in soil organic matter[15], and increases the plant's available water level by improving the water retention capability of soil, improving properties of soil[16,17]. The biochar stores carbon in the organic matter of soil, thus mediating in carbon sequestration[18]. It also helps to reduce the release of greenhouse gases in atmosphere[19]. Biochar improves water retention by increasing soil porosity and enhancing water-holding capacity, which helps plants survive during drought[20]. It also promotes nutrient cycling by enhancing microbial activity, creating a more favorable environment for microorganisms that break down organic matter and release essential nutrients like nitrogen and phosphorus[21]. These mechanisms collectively improve soil structure, water availability, and plant health, particularly under water-stress conditions. These are the reasons that give a clear win-win indication about the use of biochar for yield improvement of crops under drought conditions[22].

To augment the efficacy of utilization of biochar in soil modification, the activation of biochar is an effective approach. The activation of biochar improves its surface area, pore size, and absorption ability[23]. This process of activation can be physical[24], chemical[25], or biological[26]. Different types of gases and steam are used in physical methods to activate biochar, but they can produce some hazardous chemicals in the environment[27]. For the chemical activation of biochar, zinc chloride[28], hydrogen peroxide[29], and sodium hydroxide[30] are used. These chemicals may increase the porosity of biochar[14], but the disadvantages are cost-effectiveness and leakage of chemicals during the process. The organic activation of biochar by extracellular enzymes secreted by microbes present in vermicompost effectively increases the pore size and biochar surface area[31], While perlite is volcanic glass and further boosts the water retention capacity of biochar[32]. Together, these materials were deemed optimal for biochar activation to address soil improvement under drought conditions.

Maize is grown widely for food, medicine, and industrial purposes[33]. As per the International Production Assessment Division (IPAD) of United States Department of Agriculture (USDA), the global production of maize was 1.16 billion MT in 2022 which is 8% lower than the previous year, while Pakistan comes at 15th number in the production ranking with annual maize yield of 9.2 million MT, which is less than 1% of global maize production. Pakistan's maize yield has decreased by 9.4% (5.8 tons/ha) since the last year's yield was 6.4 tons/ha. According to USDA, the decline in corn production in the year 2022 was due to delayed planting and a recent drought scenario. Therefore, to minimize the effects of drought on food security, using activated biochar could be a beneficial approach to handle the declining yield due to water stress. Due to increased agricultural activities and crop production to fulfill the needs of food for an increasing population, the soil is becoming less fertile, and its water retention capacity is getting poor[34]. Moreover, semi-arid and arid areas are becoming vulnerable to water stress due to changing climatic patterns[35]. Therefore, an easily accessible approach should be devised that can increase the yield and, at the same time, prevent soil from degradation. Thus, using organically activated biochar for maize under drought conditions could be helpful in problems addressed earlier. Despite biochar's documented benefits, there is a significant gap in research on its practical application in field settings, especially under drought conditions in regions like Pakistan. Most existing studies focus on controlled environments, which limits our understanding of how biochar performs in real-world scenarios. This study addresses this gap by evaluating organically activated biochar in field conditions and examining its effects on maize growth, soil properties, and crop productivity. The present work addresses how does organically activated biochar influence maize's physiological and biochemical responses under varying moisture levels? The research innovatively uses comprehensive biochemical, physiological, and yield parameters to assess biochar's impact and identifies the optimal amendment levels to enhance crop productivity under water-stressed conditions.

Materials and methods

Biochar production and activation

Arabic tree (*Acacia nilotica* L.) timber chips were utilized to produce biochar. The reactor was heated at an average ramp of 20 ℃ until reaching 450 ℃, sustaining pyrolysis for three hours. The surface characteristics of biochar were further modified by the activation process, through a blend with vermicompost tea and perlite (1:1:1 ratio). For accelerated activation, a 2-liter liquid molasses solution was included, and the mixture was blended daily to clinch proper aeration. This process continued for two weeks until excess moisture disappeared, yielding a glossy black solid soil amendment[32].

Characterization of research site

The experiment was conducted in two successive years 2023–2024 to determine the optimal level of activated biochar under varying moisture conditions. The soil of the research site was a loam with little higher clay ratio (280 g/kg silt, 390 g/kg clay and 330 g/kg sand). Soil pH at the 0.00–0.15-meter layer was determined by ISO 10,390 (2021) and soil EC was determined by the method of Rayment & Higginson[36]. Elemental and structural analysis of soil samples (Fig. 1) was perfumed by SEM (scanning electron microscope) JSMS910 (JEOL, Japan). Soil saturation percentage, bulk density by core method, particle density, soil total porosity, soil organic matter, nitrogen, available potassium and phosphorus, oxidizable carbon and total organic carbon were determined by the Estefan method[37]. The initial properties of the soil indicate a loamy texture, a pH of 7.6, 0.8 ds m^{-1} EC, saturation percentage 30%, and 62% porosity, with very low organic matter (0.36%) and total carbon content (0.21%), along with moderate nutrient levels. The activated biochar exhibited a pH of 7.82, an electrical conductivity (EC) of 0.4 dS m^{-1}, a saturation percentage of 62%, and a porosity ranging from 75 to 78%. The biochar's organic matter content ranged between 0.69% and 0.85%, with a total carbon content of 0.4–0.49%.

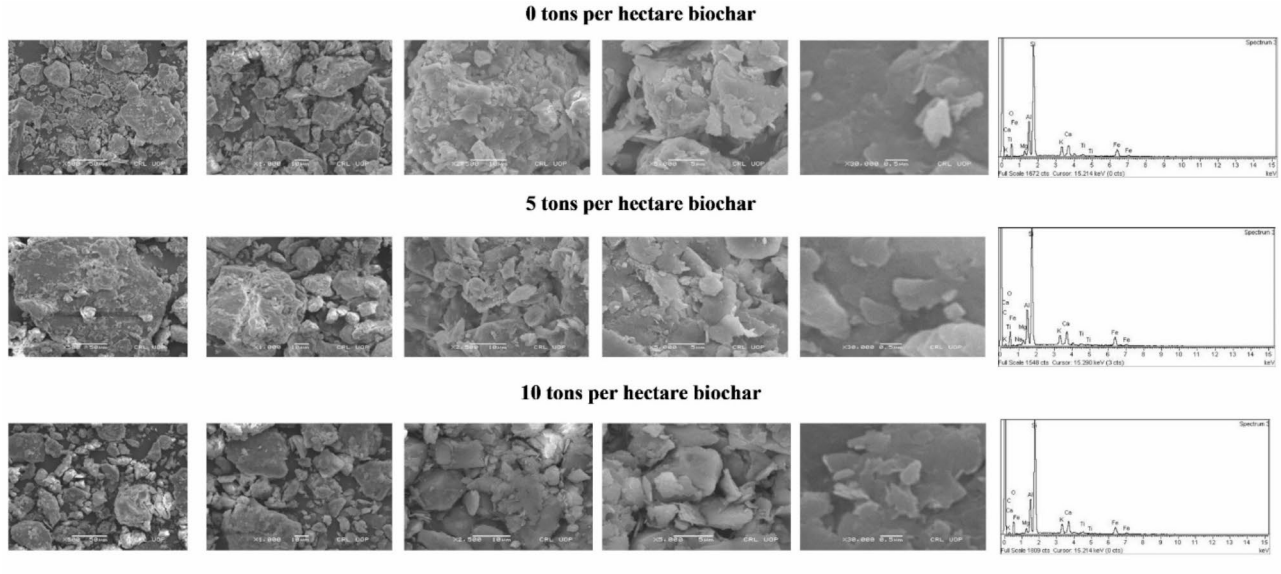

Fig. 1. SEM & EDX analysis of 0 tons/ ha, 5 tons/ha, and 10 tons/ha biochar supplemented soil showing particles, porosity and elemental composition.

Sr. No	Abbreviation	Treatment
1	T1	ETC 100%, 0 tons biochar
2	T2	ETC 80%, 0 tons biochar
3	T3	ETC 70%, 0 tons biochar
4	T4	ETC 60%, 0 tons biochar
5	T5	ETC 50%, 0 tons biochar
6	T6	ETC 100%, 5 tons biochar
7	T7	ETC 80%, 5 tons biochar
8	T8	ETC 70%, 5 tons biochar
9	T9	ETC 60%, 5 tons biochar
10	T10	ETC 50%, 5 tons biochar
11	T11	ETC 100%, 10 tons biochar
12	T12	ETC 80%, 10 tons biochar
13	T13	ETC 70%, 10 tons biochar
14	T14	ETC 60%, 10 tons biochar
15	T15	ETC 50%, 10 tons biochar

Table 1. Experiment treatments repeated in triplicates with three maize hybrid DK-9108, DK-6321 and Sarhaab. ETC is indicating evapotranspiration

The water content retention curve was fitted by using a non-linear Van Gunechten model[38] by adjusting the van Gunechtan parameters utilizing SWRC Excel solver function developed by Anlauf[39]. The saturated hydraulic conductivity was determined by constant head method (Klute 1965). The unsaturated hydraulic conductivity was estimated by the Mualem-van Genuchten Model[38].

Experiment design and treatments

The successive field experiments were managed in the village Hardaas Pur, Gujrat, Pakistan (32°38.37'N, 74°9.00'E) to determine the optimal level of activated biochar under varying moisture conditions. Maize hybrids (DK-9108, DK-6321, and Sarhaab) seeds were sourced from Bayer, Corporate Lahore, Pakistan. Biochar was applied at three levels in the 20 cm of soil top layer: no biochar (control, 0 tons per hectare), 5 tons per hectare, and 10 tons per hectare. The experiment utilized a split-plot design with 45 subplots (2 m by 2 m), each comprising three rows spaced 30 cm apart. Each maize hybrid was sown in a separate subplot, with seeds planted at a level of 3–5 cm and a frequency of 14 seeds per row. Experiment consists of 45 treatments with five moisture levels (100%, 80%, 70%, 60%, and 50% ETC) and three biochar application rates (0 t/ha, 5 t/ha, and 10 t/ha) as outlined in Table 1.

Crop water management and irrigation strategy

The crop water need was computed by the following equation projected by Food and Agriculture Organization for United States (FAO).

$$\mathrm{IN} = \mathrm{ETC} - \mathrm{Pe}$$

Where; IN is the net water requirement, ETc is crop evapotranspiration, and Pe represents effective rainfall. Moreover, the evapotranspiration was calculated by using this expression[40],

$$\mathrm{ETc} = \mathrm{ET_O} \times \mathrm{K_C}$$

ETo is reference evapotranspiration, and Kc is crop coefficient. Reference evapotranspiration was calculated by using Penman Monteith Eq. 4[41],

$$\mathrm{ETo} = \frac{0.41\Delta\ (\mathrm{RN} - \mathrm{G}) + \gamma\ [900/(\mathrm{T} + 273)]\ \mathrm{U2}\ (\mathrm{es} - \mathrm{ea})}{\Delta\ + \gamma\ (1 + 0.3\ \mathrm{U2})}$$

Where; mean daily temperature at a height of 2 meters (°C), RN symbolizes net radiation, G represents the heat flux of soil in MJm^2/day, Δ represents gradient of the vapor pressure-temperature curvature in k.Pa (°C) $^{-1}$, γ is psychometric constant ($kPa°C^{-1}$), U2 denotes daily wind rate at 2-meter elevation in meters per second, 'es' denotes the average saturation vapor pressure, while 'ea' signifies the real vapor pressure.

Calculations for ETo were performed in CROPWAT 8.0, entering geographic information (location, year, altitude (m), latitude (°), longitude (°), and weather variables including minimum temperature (°C), maximum temperature (°C), relative humidity (%), speed of wind (m/s), and sunlight hours. These variables for the experimental site were obtained from the Earth Observing System and Data Analytics (EOSDA, 2023), a satellite-based crop monitoring platform (Fig. 2). Crop stage-specific coefficients (Kc values) for maize, derived by[42], were employed in the experiment, varying from 0.35 to 1.20 based on the crop stage. Effective rainfall was estimated using the FAO/AGLW dependable rain formula in CROPWAT 8.0,

$$\mathrm{Pe} = (0.6 \times \mathrm{P}) - 3.33$$

If $P \leq 70$ mm.

Pe is effective rainfall, while P is the total precipitation in mm.

Relative growth and yield analysis

Relative increase in leaf area

The proportional growth in leaf area was deduced by the following expression by[43]

$$\text{Relative increase in leaf area} = \frac{\log_e \mathrm{L}_2 - \log_e \mathrm{L}_1}{\mathrm{T}_2 - \mathrm{T}_1}$$

L_1, Leaf area of initial harvesting, L_2, Leaf area of the next harvesting, T_1, Number of days of initial harvesting, and T_2, Number of days of the next harvesting.

For leaf area (cm^3), pictures of plant leaves were taken and processed in ImageJ software (NIH, v. 1.8.0_345 64-bit, Bethesda, MD, USA) using polygon selection in the software[44].

$$\text{Relative change in leaf fresh/dry weight} \left(\frac{\mathrm{g}}{\mathrm{day}}\right) = \frac{\log_e \mathrm{w}_2 - \log_e \mathrm{w}_1}{\mathrm{T}_2 - \mathrm{T}_1}$$

w_1, Leaf fresh weight of the initial harvesting, and w_2, Leaf fresh weight of the next harvesting.

Relative increase in shoot/root weight

The proportional expansion in root and shoot fresh and dry weight was calculated by using the following formula by[45];

$$\text{Relative increase in shoot or root fresh/dry weight} \left(\frac{\mathrm{g}}{\mathrm{day}}\right) = \frac{\log_e \mathrm{w}_2 - \log_e \mathrm{w}_1}{\mathrm{T}_2 - \mathrm{T}_1}$$

While, the fresh and dry weight of root and shoot was recorded by electrical weighing balance.

Relative growth rate

The relative growth rate was deduced by the formula given below[46],

$$\text{Relative growth rate} \left(\frac{\mathrm{g}}{\mathrm{day}}\right) = \frac{\log_e \mathrm{W}_2 - \log_e \mathrm{W}_1}{\mathrm{T}_2 - \mathrm{T}_1}$$

W_1, Initial dry matter of initial harvesting, and W_2, Initial dry matter of the next harvesting.

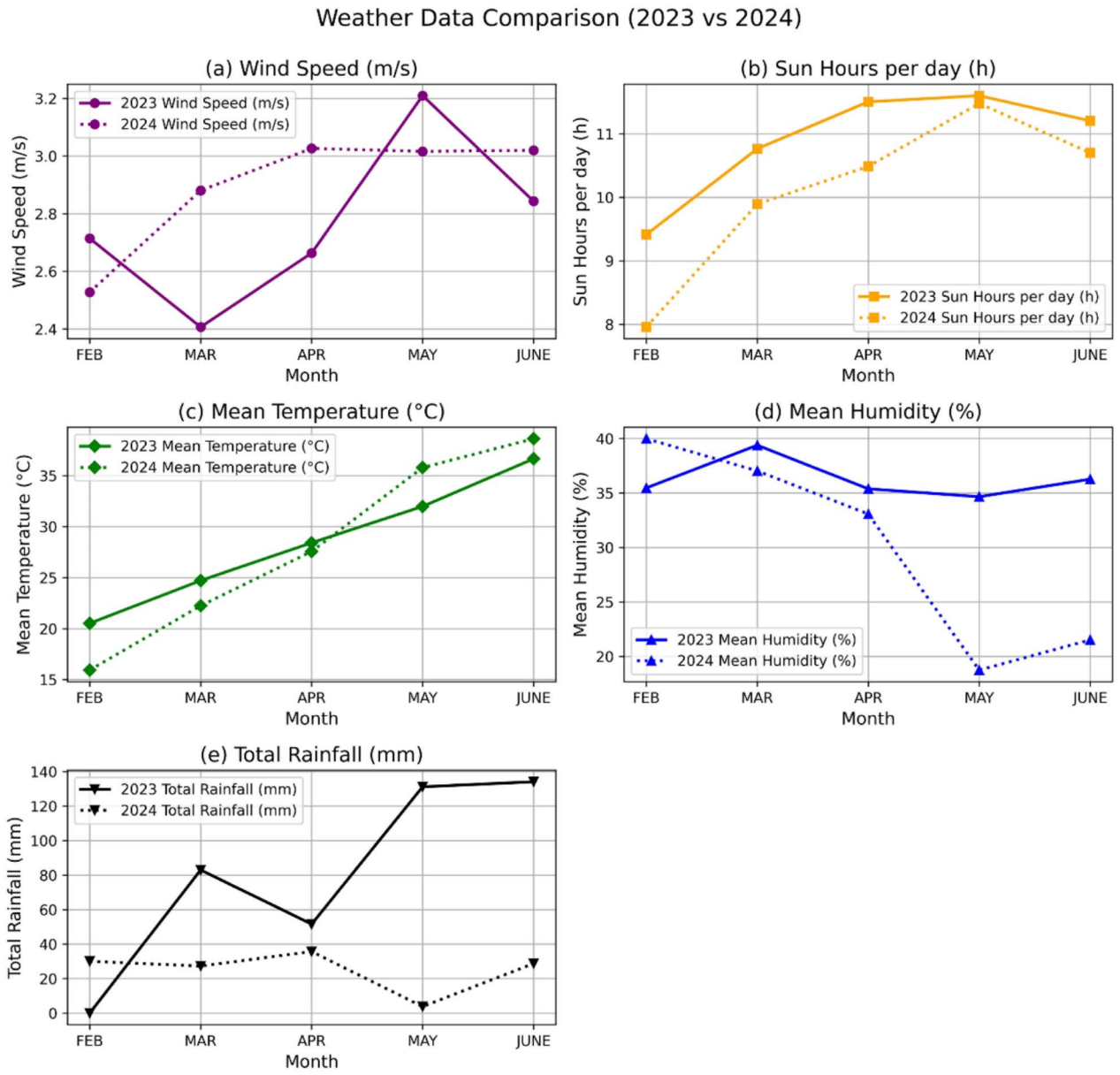

Fig. 2. Weather data comparison of experimental site during the maize seasons (2023 and 2024) obtained from Earth Observing System and Data Analytics (EOSDA) satellite-based precision agriculture platform (**a**) Wind Speed (**b**) Average sun hours per day (**c**) Mean daily temperature (**d**) Mean daily humidity (**e**) Total rainfall.

Net assimilation rate

The net assimilation rate of the maize plants was calculated by[46].

$$\text{Net assimilation rate or E}\left(\frac{\text{mg}}{\text{cm}^2}\right) = \frac{1}{\log_e L_2 - \log_e L_1} \times \frac{W_2 - W_1}{T_2 - T_1}$$

W_1, Primary dry matter of plant, W_2, Final dry matter of plant, L_1, Primary leaf area, L_2, Final leaf area, and T2 – T1, Time interval difference between harvestings.

Plant sampling for relative growth analysis was taken three times with the interval of 15 days between each sampling, starting from the starting of vegetative stage.

Physiological and biochemical analysis

Cell membrane stability index assessment

The cell membrane stability index was calculated by the method of Premachandra et al.[47], and the modifications by Sairam[48]. The Bradford's method[49] was used to find the protein content. Lipid peroxidation or malondialdehyde content in the leaf was determined by following the method of Prochazkova et al.[50]. The 2 ml of 0.1% trichloroacetic acid (TCA) was added to (100 mg) grounded leaf material. Then, the mixture was centrifuged. The top layer was separated and 4 ml of 0.5% TBA (thiobarbituric acid) and 1 ml of 20% TCA was mixed in it and warmed in a water bath for about 30 min at 95 °C. The absorbance values were noted at 600 nm, 532 nm, and 440 nm, the malondialdehyde level was evaluated by using the following formula:

$$\mathrm{MDA} = \frac{[(A_b532 - A_b600) - [(A_b440 - A_b600)\left(\frac{\text{Mol. A of Sucrose at 532 nm}}{\text{Mol. A of Sucrose at 440 nm}}\right)]}{15700} \times 10^6$$

Antioxidant activity assessment

To assess antioxidant enzyme activity, leaf material was pulverized in a clean mortar using 5 ml phosphate buffer by keeping in an ice bath. Following this, the mixture was separated at 13,000 g for 20 min at 4 °C, and the resulting top layer was analysed for antioxidant enzyme activity.

Superoxide dismutase activity

The photochemical reduction of nitro blue tetrazolium (NBT) inhibition was measured to assess the activity of SOD by using the Beauchamp & Fridovich[51] approach. Each reaction sample included 0.5 ml phosphate buffer, 0.2 ml of triton X, 0.1 ml of riboflavin (0.002 mM), 0.1 ml of enzyme extract, and 0.1 ml of methionine (13 mM). At 560 nm, the samples' absorbance was measured by UV spectrophotometer. To calculate SOD activity, the following formulas was used:

$$\mathrm{IU} = \frac{\text{absorbance}}{50} \times 100$$

IU is a global unit for enzyme activity

$$\mathrm{SOD} = \frac{\mathrm{IU}}{\text{mass of protein}}$$

Peroxidase activity

The process designated by Vetter et al.[52] was employed for the assessment of peroxidase activity, incorporating adjustments as suggested by Gorin & Heidema[53]. The reaction combination consisted of 0.2 ml of enzyme extract, 1.8 ml of a 100 mM phosphate buffer (pH 7), 0.3 ml of 3 mM H_2O_2, and 0.1 ml of an aqueous solution containing 1% w/v p-phenylenediamine. The variations' absorbance was recorded for three minutes at 485 nm by UV spectrophotometer, and the peroxidase activity was evaluated using the formula:

$$\mathrm{POD} = \frac{\Delta\, 485}{\text{mg of protein}}$$

Catalase activity

To evaluate the catalase activity within the leaf sample, a reaction blend (3 ml) was organised, consisting of 0.2 ml enzyme extract, 2.6 ml potassium phosphate buffer with a pH of 7.2, and 0.2 ml of 15 mM H_2O_2.To stop the reaction, 2 ml of titanium reagent was added after 5 min. After centrifuging, the mixture for 10 min, values of absorbance at 410 nm were taken by UV spectrophotometer. This formula was used to determine the catalase activity:

$$\mathrm{CAT} = \frac{\Delta\, 410}{\text{mg of protein}}$$

Yield analysis

After harvesting of maize crop, following yield parameters were recorded such as cob length (cm), cob weight (g), and kernel number per cob, cob yield per plant, hundred grain weight, stover yield, and apparent water productivity.

The cob length (cm) was measured by processing the images of corn cobs in a java-based software, ImageJ (NIH version 1.8.0_345 64-bit, Bethesda, MD, USA)[44]. The cob weight (g) and thousand seed weight (g) were measured by electrical weighing balance, kernel number per cob were counted manually. Stover yield was calculated as the dry biomass after harvesting the cobs.

The grain yield of a plant was estimated by taking the weight of seeds per cob. Further, yield per hectare was estimated by multiplying the plant density according to layout by grain yield per plant.

$$\mathrm{Yield}\left(\frac{\mathrm{kg}}{\mathrm{ha}}\right) = \text{Grain yield per plant} \times \text{planting density}$$

$$\text{Planting density per hectare} = \frac{\text{Area of plot } (\text{m}^2)}{\text{R} - \text{R Spacing } (\text{m}^2)}$$

The next formula was used to calculate the evident water productivity by following Shabbir et al.[54]

$$\text{Apparent water productivity } \left(\text{kg}/m^3\right) = \text{AWP} = \frac{\text{Grain Yield (kg)}}{\text{Irrigation water supply } (m^3)}$$

Statistical analysis

The statistical analyses for the study were executed by using Minitab software (Ver. 21.2). Three-Way Analysis of Variance (ANOVA) in the framework of a General Linear Model (GLM) was employed to measure the influence of various growth, biochemical, physiological, and yield attributes. The main purpose of this analysis was to observe how the factors of amendments, evapotranspiration (ETC) levels, and maize hybrid influenced the growth, biochemical, and yield related parameters. To further explore significant differences among factor levels, Tukey Pairwise Comparison tests with a 95% Confidence Interval were conducted. This post-hoc analysis allowed a detailed examination of specific differences between factor levels while maintaining a high level of confidence. The covariance and correlation analysis of variables were performed in Visual Studio Code using Python libraries (kernel = Python 3.11.9) by constructing Principal Component Analysis (PCA) biplot and heatmap.

Results

Soil characterization

The results of soil physicochemical properties are presented in Table 2. Soil bulk density and particle density were considerably lower (13–23%; 9–23%) in 5 T/ha and 10 T/ha biochar supplemented soil respectively. However, the highest total porosity was recorded in soil amended with 10 tons/ha biochar amended soil that is 26% higher than the soil with no biochar supplementation. The EC (13-45%), organic matter, nitrogen, total organic carbon and oxidizable carbon significantly enhanced with biochar supplementation in the soil by 87–130%. Similarly, available phosphorus (5-9%) and potassium (26–34%) also improved considerably in biochar supplemented soil. Biochar supplementation in soil caused no significant effects on C/N ratio but caused a bit increase in pH from 7.6 to 7.9 in contrast to non-supplemented soil. The SEM-EDX analysis of soil mineral profile indicates a considerable improvement in O, C, Mg, Si, K, Ca, and Fe by 17.3–21%, 34–63%, 3-7.3%, 2–4%, 2–7%, 1–5%, and 7–8% in 5 tons/ha and 10 T/ha biochar supplemented soil, respectively, in contrast to soil without biochar supplantation. However, titanium content decreased in biochar supplemented soil. The SEM images of the soil samples also (Fig. 1) revealed an array of macro, meso and micropores in biochar supplemented soil. The water content (cm^3/cm^3) at five pressure heads was determined by pressure plates extractors and the fitted curve

Parameter	0 Tons per hectare	5 Tons per hectare	10 Tons per hectare
Saturation percentage (%)	30 ± 2 (c)	35 ± 1.5 (b)	40 ± 1.16 (a)
Bulk density (Mg m^{-3})	1.75 ± 0.042 (a)	1.53 ± 0.036 (b)	1.38 ± 0.05 (c)
Particle density (Mg m^{-3})	2.84 ± 0.22 (a)	2.58 ± 0.16 (b)	2.18 ± 0.28 (c)
Total porosity (%)	62 ± 5.2 (c)	75 ± 4.7 (ab)	78 ± 1.3 (a)
EC (ds m^{-1})	0.827 ± 0.031 (c)	0.93 ± 0.03 (b)	1.2 ± 0.13 (a)
pH	7.63 ± 0.015 (b)	7.68 ± 0.015 (b)	7.97 ± 0.06 (a)
Organic matter (%)	0.363 ± 0.032 (c)	0.69 ± 0.01 (b)	0.85 ± 0.06 (a)
Available phosphorus (mg kg^{-1})	6.67 ± 0.15 (b)	7 ± 0.06 (a)	7.3 ± 0.1 (a)
Available potassium (mg kg^{-1})	62.3 ± 2.5 (b)	78 ± 1 (a)	83 ± 2.7 (a)
Total organic carbon (%)	0.21 ± 0.019 (c)	0.4 ± 0.0058 (b)	0.49 ± 0.037 (a)
Oxidizable carbon (%)	0.158 ± 0.014 (c)	0.3 ± 0.004 (b)	0.37 ± 0.028 (a)
Nitrogen (%)	0.024 ± 0.002 (c)	0.046 ± 0.0001 (b)	0.056 ± 0.004 (a)
Oxygen (%)	20.55 ± 1.21 (b)	24.1 ± 0.95 (a)	24.89 ± 1.32 (a)
Carbon (%)	4.8 ± 0.13 (c)	6.42 ± 0.21 (b)	7.82 ± 0.14 (a)
Magnesium (%)	1.51 ± 0.04 (c)	1.56 ± 0.062 (ab)	1.62 ± 0.01 (a)
Aluminum (%)	10.05 ± 0.02 (a)	9.31 ± 0.01 (b)	10.05 ± 0.031 (a)
Silicon (%)	38.17 ± 0.45 (b)	39.06 ± 0.54 (a)	39.57 ± 0.47 (a)
Potassium (%)	4.43 ± 0.035 (c)	4.51 ± 0.034 (bc)	4.75 ± 0.047 (a)
Calcium (%)	6.26 ± 0.023 (b)	6.29 ± 0.032 (b)	6.56 ± 0.04 (a)
Titanium (%)	1.083 ± 0.12 (a)	0.85 ± 0.028 (b)	0.93 ± 0.032 (b)
Ferric (%)	9.18 ± 0.15 (c)	9.82 ± 0.02 (ab)	9.895 ± 0.013 (a)
Carbon/nitrogen ratio	8.75 ± 0.09 (a)	8.7 ± 0.12 (ab)	8.75 ± 0.17 (a)

Table 2. Physicochemical and nutrient status of soil. ± value indicates standard error of three replicates while different letter in parenthesis indicates significant differences at 95% confidence interval.

(from pF 0 to pF 4.5) is shown in Fig. 3a. The biochar supplemented treatments showed more water retention content as compared to non-biochar supplemented one. The mean saturated hydraulic conductivity is seemed to be decreased in biochar amendments as compared to control. 66.72 cm/day, 43.83 cm/day, and 51.30 cm/day saturated hydraulic conductivity has been noted in 0 tons/ha, 5 tons/ha and 10 tons/ha treatments respectively. The fitted curve for unsaturated hydraulic conductivity is represented in Fig. 3b.

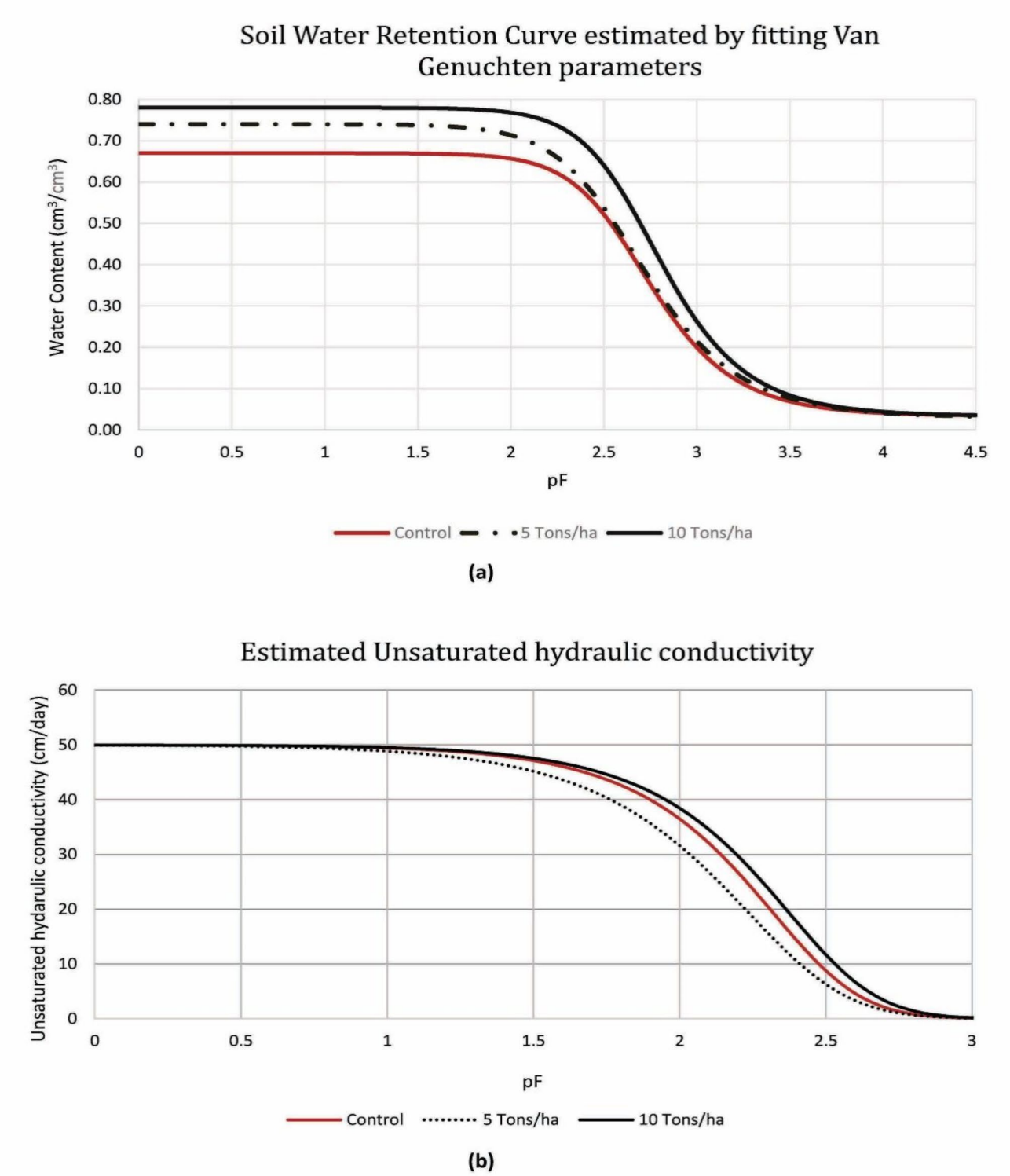

Fig. 3. (**a**) Estimation of Soil Water Retention Curve fitted by van Genuchten model parameters adjustments (**b**) Unsaturated hydraulic conductivity curve fitted by using the Mualem-van Genuchten Model.

Crop water balance

The water balance of maize during the spring seasons is pictured in Fig. 4. The effective rainfall during the season was 102.95 mm in 2023 season, and only 5.78 mm in 2024. The total water deficit during the crop duration was 576.8 mm in 2023 season, and 714.73 mm in 2024 season. The water deficit met by manual irrigation by 576.8 mm, 453.2 mm, 391.3 mm, 329.5 mm, and 267.7 mm in 2023 season, and 714.73 mm, 573.97 mm, 503.59 mm, 433.21 mm, 362.83 mm in 2024 season, respectively in 100% ETC, 80% ETC, 70% ETC, 60% ETC, and 50% ETC sub-plots. The water deficit is dependent on the environmental conditions as well as crop coefficient (stage of crop growth). It has been seen that the highest water deficit from the crop was noticed at the dough stage in both seasons (12th week on charts) where the crop coefficient was highest (Kc = 1.20) with the counteract of other variables, like humidity, temperature, wind speed, and sunlight duration.

Relative growth analysis

The relative growth in fresh and dry weight of maize roots and shoots is summarized in Table 3. Water stress conditions led to a notable decrease in the relative weight gain of maize roots and shoots. However, soils enriched with biochar exhibited significantly improved results, with a 42% increase in root weight and a 34% increase in shoot weight. Notably, treatments at 80% ETC showed a greater relative increase in root and shoot weight compared to the 100%, 70%, 60%, and 50% ETC levels, with improvements of 1.02, 1.09, 1.51, and 1.97 times, respectively. The highest relative increase in fresh and dry weight of the maize plant was observed in the DK-6321 variety, cultivated in soil amended with 5 tons/ha of biochar under 80% ETC conditions. This resulted in a 1.68-fold increase over its respective control treatment.

Table 4 highlights the significant variations in the relative increase in maize leaf weight and leaf area ($P < 0.05$). Similar to the root and shoot findings, water stress reduced the relative gains in leaf weight and area. However, plants grown in biochar-supplemented soil outperformed the control, showing a 45% higher leaf weight and a 54% increase in leaf area. Additionally, 80% ETC treatments outperformed the other water regimes, improving leaf weight by 1.15, 1.18, 1.71, and 2.27 times, and leaf area by 1.11, 1.20, 1.70, and 2.47 times, for 100%, 70%, 60%, and 50% ETC, respectively. The maximum increase in maize leaf weight and leaf area was again seen in the DK-6321 variety, cultivated in 5 tons/ha biochar-amended soil under 80% ETC conditions, showing a 2.05-fold increase in comparison to its control treatment.

Furthermore, the net assimilation rate (NAR) and relative growth rate (RGR) for maize hybrids are displayed in Table 4. Water stress had a detrimental effect on both NAR and RGR, while biochar-supplemented treatments led to improvements, boosting NAR by 46% and RGR by 35%. As with other parameters, the 80% ETC treatments outperformed other ETC levels, increasing NAR by 1.14, 1.13, 1.57, and 2.27 times, and RGR by 1.17, 1.08, 1.31, and 1.66 times compared to 100%, 70%, 60%, and 50% ETC, respectively. The highest values for both NAR and RGR were found in the DK-6321 variety, cultivated in 5 tons/ha biochar-amended soil at 80% ETC, with NAR increasing 2.10 times and RGR rising 1.76 times compared to its control treatment. Among the three maize hybrids, DK-6321 consistently led in all relative growth parameters, followed by Sarhaab and DK-9108.

Biochemical and physiological parameters

The analysis of variance for biochemical and physiological parameters at both the vegetative and reproductive stages revealed significant outcomes (Tables 5 and 6).

At the vegetative stage, biochar-amended soil showed significantly enhanced physiological and biochemical attributes compared to non-amended soil. The maize grown in biochar-supplemented soil exhibited 1.62 times higher membrane stability index (MSI), 1.43 times more protein content, and increased antioxidant enzyme activities, with superoxide dismutase (SOD) up by 1.47 times, peroxidase (POD) by 1.24 times, and catalase (CAT) by 1.21 times. In contrast, malondialdehyde (MDA) levels were substantially higher in non-amended maize, with a 0.63-fold increase compared to biochar-treated maize. When comparing different ETC levels, the 80% ETC treatments resulted in greater MSI and protein content, with MSI increasing by 1.01, 1.11, 1.33, and 1.72 times, and protein content rising by 1.21, 1.15, 1.62, and 2.05 times compared to 100%, 70%, 60%, and 50% ETC, respectively. However, MDA levels, as well as SOD, POD, and CAT activity, were highest under 50% ETC, with MDA increasing by 1.46, 1.32, 1.23, and 1.16 times over 100%, 80%, 70%, and 60% ETC. Similarly, SOD, POD, and CAT activity at 50% ETC were elevated by 4.39, 3.63, 2.75, and 1.51 times, 4.54, 3.73, 2.85, and 1.44 times, and 2.49, 2.02, 1.76, and 1.46 times, respectively, compared to the other ETC levels.

At the reproductive stage, biochar amendments again resulted in higher MSI, protein content, and antioxidant enzyme activities. Maize grown in biochar-enriched soil had 1.61 times higher MSI, 1.39 times more protein content, and increased SOD, POD, and CAT activities by 1.13, 1.38, and 1.22 times, respectively, compared to non-amended maize. MDA content was higher in non-biochar-amended plants, with an 77% increase compared to biochar-amended ones. The ETC comparison at the reproductive stage mirrored the vegetative stage findings, with 80% ETC treatments leading to improvements in MSI (by 1.17, 1.12, 1.33, and 1.70 times) and protein content (by 1.20, 1.14, 1.53, and 2.01 times) compared to 100%, 70%, 60%, and 50% ETC. The 50% ETC showed the highest MDA levels, with increases of 1.37, 1.28, 1.22, and 1.14 times compared to the other ETC treatments. The 50% ETC also showed significantly higher SOD activity (by 2.95, 2.43, 1.75, and 1.24 times), POD activity (by 3.52, 2.85, 2.28, and 1.40 times), and CAT activity (by 2.15, 1.99, 1.73, and 1.35 times) compared to 100%, 80%, 70%, and 60% ETC.

Across both stages, the 5 tons/ha biochar amendment consistently exhibited superior responses in biochemical and physiological parameters compared to 10 tons/ha and 0 tons/ha treatments. Among the ETC levels, 80% ETC proved to be the most effective, outperforming 100%, 70%, 60%, and 50% ETC. In terms of maize varieties, DK-6321 showed the best performance, followed by Sarhaab and DK-9108.

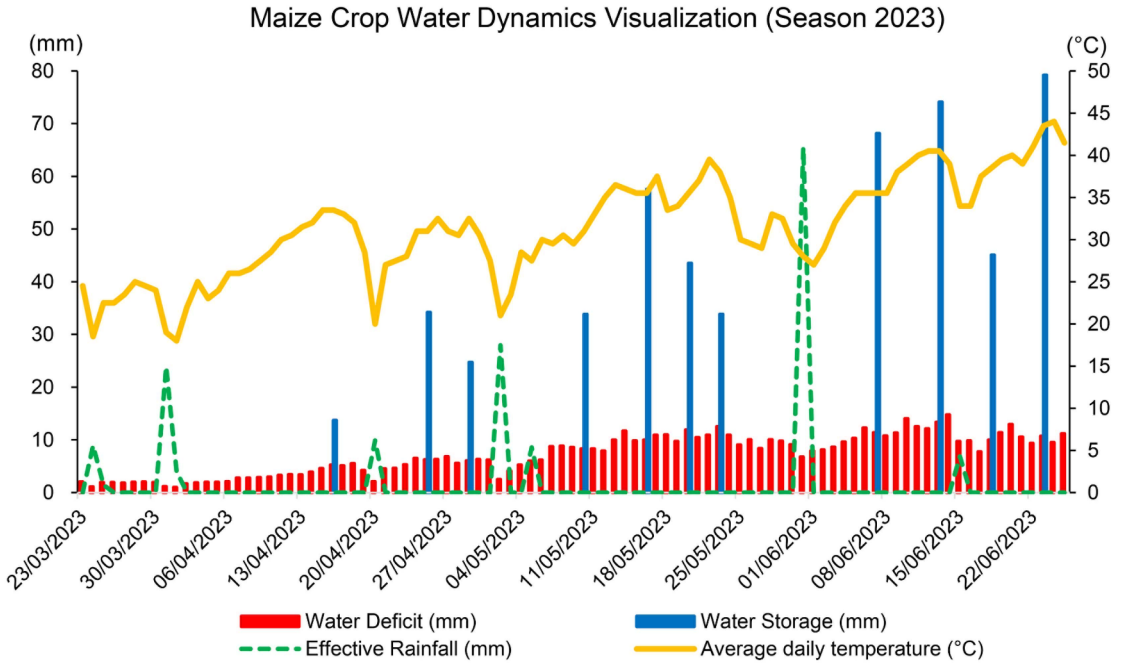

(b)

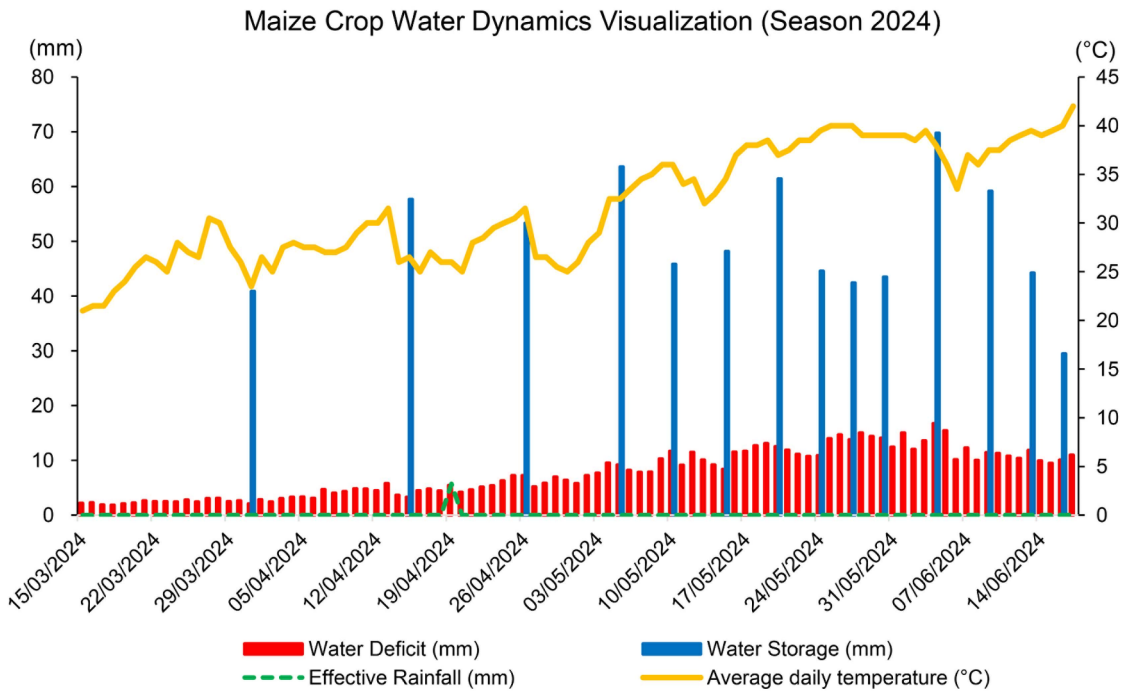

Fig. 4. Visualization of maize crop water dynamics during the crop growing seasons by using data from the EOSDA crop monitoring platform (**a**) Season 2023 (23rd March to 25th June), (**b**) Season 2024 (15th March to 17th June).

Treatment	Relative increase in root fresh weight (g/day)	Relative increase in root dry weight (g/day)	Relative increase in shoot fresh weight (g/day)	Relative increase in shoot dry weight (g/day)
V1, E 100%, 0T	0.088 ± 0.002 (k-m)	0.086 ± 0.002 (k-m)	0.099 ± 0.002 (k)	0.098 ± 0.002 (k)
V1, E 80%, 0 T	0.069 ± 0.003 (q-s)	0.067 ± 0.003 (q-s)	0.069 ± 0.002 (o-q)	0.067 ± 0.002 (o-q)
V1, E 70%, 0 T	0.05 ± 0.003 (u-w)	0.049 ± 0.003 (v-x)	0.06 ± 0.003 (q-r)	0.058 ± 0.003 (q-r)
V1, E 60%, 0 T	0.046 ± 0.003 (v-w)	0.045 ± 0.003 (w-x)	0.049 ± 0.002 (u-v)	0.047 ± 0.002 (u-v)
V1, E 50%, 0 T	0.033 ± 0.002 (x)	0.032 ± 0.001 (y)	0.037 ± 0.003 (x)	0.036 ± 0.003 (x)
V1, E 100%, 5 T	0.102 ± 0.002 (g-j)	0.101 ± 0.002 (g-j)	0.106 ± 0.003 (h-k)	0.105 ± 0.003 (h-k)
V1, E 80%, 5 T	0.119 ± 0.003 (a-c)	0.117 ± 0.003 (a-c)	0.122 ± 0.003 (b-e)	0.121 ± 0.002 (b-e)
V1, E 70%, 5 T	0.108 ± 0.002 (d-h)	0.106 ± 0.001 (d-h)	0.115 ± 0.003 (e-h)	0.114 ± 0.001 (e-h)
V1, E 60%, 5 T	0.081 ± 0.003 (m-o)	0.08 ± 0.003 (m-o)	0.074 ± 0.003 (m-o)	0.073 ± 0.001 (m-o)
V1, E 50%, 5 T	0.066 ± 0.003 (r-s)	0.065 ± 0.002 (r-s)	0.05 ± 0.002 (t-v)	0.049 ± 0.002 (t-v)
V1, E 100%, 10 T	0.095 ± 0.003 (j-k)	0.094 ± 0.003 (j-k)	0.101 ± 0.002 (j-k)	0.1 ± 0.003 (j-k)
V1, E 80%, 10 T	0.111 ± 0.003 (c-g)	0.109 ± 0.003 (c-g)	0.117 ± 0.003 (d-g)	0.115 ± 0.003 (d-g)
V1, E 70%, 10 T	0.103 ± 0.003 (f-j)	0.102 ± 0.003 (f-j)	0.108 ± 0.003 (g-j)	0.107 ± 0.002 (g-j)
V1, E 60%, 10 T	0.074 ± 0.003 (o-r)	0.073 ± 0.003 (o-r)	0.063 ± 0.003 (p-r)	0.062 ± 0.002 (p-r)
V1, E 50%, 10 T	0.055 ± 0.002 (t-v)	0.053 ± 0.002 (t-w)	0.041 ± 0.003 (v-x)	0.04 ± 0.002 (v-x)
V2, E 100%, 0 T	0.097 ± 0.003 (i-k)	0.095 ± 0.004 (i-k)	0.108 ± 0.003 (h-k)	0.106 ± 0.004 (h-k)
V2, E 80%, 0 T	0.078 ± 0.003 (n-q)	0.076 ± 0.003 (n-q)	0.082 ± 0.003 (l-m)	0.08 ± 0.002 (l-m)
V2, E 70%, 0 T	0.062 ± 0.002 (s-t)	0.061 ± 0.002 (s-t)	0.072 ± 0.003 (n-p)	0.071 ± 0.003 (n-p)
V2, E 60%, 0 T	0.057 ± 0.002 (t-u)	0.055 ± 0.002 (t-v)	0.064 ± 0.003 (p-r)	0.063 ± 0.004 (p-r)
V2, E 50%, 0 T	0.049 ± 0.003 (u-w)	0.048 ± 0.003 (v-x)	0.045 ± 0.002 (u-x)	0.043 ± 0.002 (u-x)
V2, E 100%, 5 T	0.112 ± 0.003 (c-f)	0.11 ± 0.002 (c-f)	0.119 ± 0.003 (d-f)	0.118 ± 0.003 (d-f)
V2, E 80%, 5 T	0.128 ± 0.003 (a)	0.126 ± 0.003 (a)	0.136 ± 0.003 (a)	0.134 ± 0.004 (a)
V2, E 70%, 5 T	0.116 ± 0.002 (b-d)	0.115 ± 0.002 (b-d)	0.129 ± 0.003 (a-c)	0.128 ± 0.003 (a-c)
V2, E 60%, 5 T	0.09 ± 0.002 (k-l)	0.089 ± 0.002 (k-l)	0.087 ± 0.003 (l)	0.085 ± 0.004 (l)
V2, E 50%, 5 T	0.075 ± 0.003 (o-q)	0.074 ± 0.003 (o-q)	0.071 ± 0.002 (o-p)	0.069 ± 0.002 (o-p)
V2, E 100%, 10 T	0.105 ± 0.002 (e-i)	0.103 ± 0.003 (e-i)	0.114 ± 0.003 (e-h)	0.112 ± 0.003 (e-h)
V2, E 80%, 10 T	0.116 ± 0.003 (b-d)	0.115 ± 0.003 (b-d)	0.125 ± 0.003 (b-d)	0.123 ± 0.003 (b-d)
V2, E 70%, 10 T	0.11 ± 0.003 (c-g)	0.109 ± 0.003 (c-h)	0.119 ± 0.003 (d-f)	0.118 ± 0.004 (d-f)
V2, E 60%, 10 T	0.082 ± 0.002 (l-o)	0.08 ± 0.002 (l-o)	0.072 ± 0.003 (n-p)	0.07 ± 0.003 (n-p)
V2, E 50%, 10 T	0.069 ± 0.002 (p-s)	0.068 ± 0.002 (p-s)	0.059 ± 0.001 (r-t)	0.058 ± 0.001 (r-t)
V3, E 100%, 0 T	0.091 ± 0.002 (k-l)	0.089 ± 0.003 (k-l)	0.104 ± 0.003 (i-k)	0.102 ± 0.004 (i-k)
V3, E 80%, 0 T	0.061 ± 0.003 (s-t)	0.059 ± 0.003 (s-u)	0.075 ± 0.003 (m-o)	0.074 ± 0.003 (l-n)
V3, E 70%, 0 T	0.055 ± 0.003 (t-v)	0.054 ± 0.002 (t-w)	0.066 ± 0.003 (o-r)	0.065 ± 0.002 (o-r)
V3, E 60%, 0 T	0.052 ± 0.003 (u-v)	0.05 ± 0.002 (u-w)	0.051 ± 0.003 (s-t)	0.049 ± 0.003 (s-u)
V3, E 50%, 0 T	0.042 ± 0.003 (w)	0.041 ± 0.003 (x)	0.04 ± 0.003 (w-x)	0.038 ± 0.003 (w-x)
V3, E 100%, 5 T	0.104 ± 0.003 (e-j)	0.102 ± 0.003 (e-j)	0.113 ± 0.002 (e-h)	0.112 ± 0.001 (e-h)
V3, E 80%, 5 T	0.122 ± 0.003 (a-b)	0.12 ± 0.003 (a-b)	0.13 ± 0.002 (a-b)	0.128 ± 0.002 (a-b)
V3, E 70%, 5 T	0.113 ± 0.003 (b-e)	0.111 ± 0.003 (b-e)	0.124 ± 0.003 (b-d)	0.123 ± 0.003 (b-d)
V3, E 60%, 5 T	0.085 ± 0.003 (l-n)	0.083 ± 0.003 (l-n)	0.08 ± 0.003 (l-n)	0.079 ± 0.003 (l-m)
V3, E 50%, 5 T	0.071 ± 0.004 (p-r)	0.07 ± 0.004 (p-r)	0.059 ± 0.002 (r-s)	0.058 ± 0.003 (r-s)
V3, E 100%, 10 T	0.101 ± 0.003 (h-j)	0.1 ± 0.003 (h-j)	0.107 ± 0.003 (h-k)	0.106 ± 0.003 (h-k)
V3, E 80%, 10 T	0.112 ± 0.003 (c-e)	0.111 ± 0.003 (c-e)	0.12 ± 0.003 (c-f)	0.119 ± 0.003 (c-f)
V3, E 70%, 10 T	0.106 ± 0.003 (e-i)	0.104 ± 0.002 (e-i)	0.112 ± 0.003 (f-i)	0.111 ± 0.003 (f-i)
V3, E 60%, 10 T	0.078 ± 0.003 (n-p)	0.077 ± 0.004 (n-p)	0.068 ± 0.002 (o-r)	0.066 ± 0.003 (o-r)
V3, E 50%, 10 T	0.061 ± 0.003 (s-t)	0.06 ± 0.003 (s-t)	0.049 ± 0.003 (u-w)	0.047 ± 0.003 (u-w)

Table 3. Impact of activated acacia wood biochar amendment on relative increase in root and shoot growth of three maize hybrids under varied moisture conditions. Note: The different letters in parenthesis after standard deviation represent significant variations among the treatments, as determined by the Tukey test and 95% confidence interval. Abbreviations: V1; DK-9108, V2; DK-6321, V3; Sarhaab, E; Evapotranspiration, T; tons biochar per hectare

Treatment	Relative increase in leaf fresh weight (g/day)	Relative increase in leaf dry weight (g/day)	Relative increase in leaf area (cm^2/day)	NAR (g cm^{-2} day^{-1})	RGR (g/day)
V1, E 100%, 0 T	0.043 ± 0.002 (j-k)	0.042 ± 0.002 (l-m)	0.032 ± 0.001 (n-p)	4.61 ± 0.215 (m-o)	0.071 ± 0.004 (j-q)
V1, E 80%, 0 T	0.035 ± 0.003 (l-o)	0.033 ± 0.002 (n-q)	0.025 ± 0.001 (s-u)	3.95 ± 0.207 (i-k)	0.061 ± 0.004 (p-t)
V1, E 70%, 0 T	0.031 ± 0.002 (n-r)	0.029 ± 0.002 (p-t)	0.019 ± 0.001 (v-x)	3.74 ± 0.225 (l-n)	0.057 ± 0.005 (r-u)
V1, E 60%, 0 T	0.026 ± 0.002 (p-s)	0.025 ± 0.002 (s-u)	0.015 ± 0.001 (y-aa)	2.94 ± 0.132 (x)	0.051 ± 0.005 (t-v)
V1, E 50%, 0 T	0.02 ± 0.002 (s)	0.019 ± 0.002 (u)	0.01 ± 0.001 (ab)	2.35 ± 0.246 (u-x)	0.035 ± 0.003 (w)
V1, E 100%, 5 T	0.056 ± 0.003 (g-i)	0.053 ± 0.002 (i-k)	0.039 ± 0.001 (j-m)	6.37 ± 0.291 (w-x)	0.082 ± 0.003 (h-j)
V1, E 80%, 5 T	0.072 ± 0.002 (c-d)	0.071 ± 0.002 (c-e)	0.054 ± 0.001 (c-e)	8.14 ± 0.123 (u-x)	0.111 ± 0.003 (a-c)
V1, E 70%, 5 T	0.06 ± 0.002 (f-h)	0.058 ± 0.002 (g-i)	0.042 ± 0.001 (i-k)	7.62 ± 0.16 (r-v)	0.097 ± 0.005 (d-f)
V1, E 60%, 5 T	0.038 ± 0.001 (k-m)	0.037 ± 0.001 (m-o)	0.029 ± 0.001 (p-r)	4.25 ± 0.228 (t-w)	0.077 ± 0.004 (h-n)
V1, E 50%, 5 T	0.031 ± 0.002 (m-r)	0.029 ± 0.002 (p-t)	0.018 ± 0.001 (w-z)	3.17 ± 0.176 (p-t)	0.066 ± 0.005 (l-r)
V1, E 100%, 10 T	0.052 ± 0.003 (i)	0.051 ± 0.002 (j-k)	0.036 ± 0.001 (m-n)	5.33 ± 0.262 (o-r)	0.075 ± 0.004 (i-o)
V1, E 80%, 10 T	0.063 ± 0.003 (e-g)	0.061 ± 0.002 (f-h)	0.048 ± 0.001 (f-g)	7.45 ± 0.264 (p-t)	0.095 ± 0.004 (d-g)
V1, E 70%, 10 T	0.054 ± 0.002 (h-i)	0.052 ± 0.002 (i-k)	0.038 ± 0.001 (k-m)	5.78 ± 0.204 (o-r)	0.089 ± 0.003 (e-h)
V1, E 60%, 10 T	0.032 ± 0.002 (m-p)	0.031 ± 0.002 (o-s)	0.024 ± 0.001 (s-u)	3.72 ± 0.14 (n-p)	0.071 ± 0.003 (j-q)
V1, E 50%, 10 T	0.025 ± 0.002 (q-s)	0.023 ± 0.001 (t-u)	0.013 ± 0.001 (aa-ab)	2.74 ± 0.28 (o-r)	0.046 ± 0.005 (u-w)
V2, E 100%, 0 T	0.051 ± 0.002 (i)	0.049 ± 0.002 (j-k)	0.043 ± 0.001 (h-i)	5.9 ± 0.262 (k-m)	0.076 ± 0.004 (h-o)
V2, E 80%, 0 T	0.043 ± 0.002 (j-k)	0.042 ± 0.002 (l-m)	0.031 ± 0.002 (o-q)	4.35 ± 0.242 (i)	0.067 ± 0.005 (k-r)
V2, E 70%, 0 T	0.038 ± 0.003 (k-m)	0.036 ± 0.002 (m-o)	0.027 ± 0.001 (q-t)	3.92 ± 0.256 (i-k)	0.064 ± 0.003 (o-s)
V2, E 60%, 0 T	0.031 ± 0.002 (m-q)	0.029 ± 0.002 (p-t)	0.021 ± 0.001 (u-w)	3.36 ± 0.22 (v-x)	0.059 ± 0.005 (q-u)
V2, E 50%, 0 T	0.027 ± 0.001 (p-s)	0.026 ± 0.001 (r-t)	0.016 ± 0.001 (x-aa)	2.85 0.302 (t-w)	0.05 ± 0.002 (t-v)
V2, E 100%, 5 T	0.066 ± 0.002 (d-f)	0.065 ± 0.002 (e-g)	0.055 ± 0.001 (c-d)	7.7 ± 0.209 (u-x)	0.097 ± 0.004 (d-f)
V2, E 80%, 5 T	0.089 ± 0.003 (a)	0.087 ± 0.002 (a)	0.063 ± 0.001 (a)	9.15 ± 0.143 (p-t)	0.118 ± 0.003 (a)
V2, E 70%, 5 T	0.075 ± 0.001 (b-c)	0.074 ± 0.002 (b-d)	0.058 ± 0.002 (b-c)	8.45 ± 0.256 (j-l)	0.106 ± 0.004 (a-d)
V2, E 60%, 5 T	0.053 ± 0.003 (h-i)	0.052 ± 0.002 (i-k)	0.04 ± 0.002 (i-l)	6.45 ± 0.249 (n-p)	0.085 ± 0.005 (f-i)
V2, E 50%, 5 T	0.035 ± 0.002 (l-n)	0.034 ± 0.002 (n-p)	0.031 ± 0.002 (o-q)	3.91 ± 0.277 (i-k)	0.078 ± 0.005 (h-m)
V2, E 100%, 10 T	0.062 ± 0.003 (e-g)	0.061 ± 0.002 (f-h)	0.051 ± 0.002 (e-g)	6.35 ± 0.126 (f-g)	0.084 ± 0.005 (g-i)
V2, E 80%, 10 T	0.077 ± 0.002 (b-c)	0.076 ± 0.001 (b-c)	0.058 ± 0.002 (b-c)	8.32 ± 0.202 (i-j)	0.107 ± 0.004 (a-d)
V2, E 70%, 10 T	0.066 ± 0.003 (d-f)	0.065 ± 0.002 (e-g)	0.047 ± 0.001 (g-h)	7.37 ± 0.169 (e-g)	0.11 ± 0.003 (a-c)
V2, E 60%, 10 T	0.043 ± 0.002 (j-k)	0.042 ± 0.002 (l-m)	0.036 ± 0.002 (l-m)	5.36 ± 0.282 (b-d)	0.079 ± 0.003 (h-k)
V2, E 50%, 10 T	0.033 ± 0.002 (m-p)	0.031 ± 0.002 (o-r)	0.024 ± 0.002 (s-u)	3.13 ± 0.205 (c-g)	0.066 ± 0.005 (m-r)
V3, E 100%, 0 T	0.049 ± 0.002 (i-j)	0.047 ± 0.002 (k-l)	0.036 ± 0.002 (l-m)	4.91 ± 0.25 (i)	0.074 ± 0.004 (i-p)
V3, E 80%, 0 T	0.04 ± 0.001 (k-l)	0.039 ± 0.001 (m-n)	0.027 ± 0.001 (q-t)	4 ± 0.197 (d-g)	0.064 ± 0.004 (o-s)
V3, E 70%, 0 T	0.035 ± 0.002 (l-n)	0.034 ± 0.002 (n-p)	0.023 ± 0.002 (t-v)	3.8 ± 0.175 (g-h)	0.061 ± 0.003 (q-t)
V3, E 60%, 0 T	0.029 ± 0.002 (n-r)	0.027 ± 0.002 (q-t)	0.019 ± 0.002 (w-y)	3.16 ± 0.252 (s-w)	0.065 ± 0.003 (n-s)
V3, E 50%, 0 T	0.024 ± 0.003 (r-s)	0.023 ± 0.002 (t-u)	0.014 ± 0.002 (z-aa)	2.5 ± 0.149 (o-s)	0.039 ± 0.003 (v-w)
V3, E 100%, 5 T	0.064 ± 0.002 (e-f)	0.062 ± 0.002 (f-g)	0.044 ± 0.002 (h-i)	7.12 ± 0.253 (q-u)	0.078 ± 0.002 (h-m)
V3, E 80%, 5 T	0.08 ± 0.003 (b)	0.078 ± 0.002 (b)	0.06 ± 0.002 (a-b)	8.55 ± 0.215 (n-q)	0.113 ± 0.004 (a-b)
V3, E 70%, 5 T	0.068 ± 0.003 (d-e)	0.066 ± 0.002 (e-f)	0.051 ± 0.002 (e-g)	7.97 ± 0.252 (h-i)	0.099 ± 0.004 (c-e)
V3, E 60%, 5 T	0.049 ± 0.003 (i-j)	0.048 ± 0.002 (k-l)	0.035 ± 0.001 (m-o)	5.73 ± 0.143 (i-k)	0.08 ± 0.004 (h-j)
V3, E 50%, 5 T	0.033 ± 0.002 (m-p)	0.031 ± 0.002 (o-r)	0.025 ± 0.001 (r-u)	3.57 ± 0.211 (d-g)	0.071 ± 0.003 (j-q)
V3, E 100%, 10 T	0.056 ± 0.002 (g-i)	0.055 ± 0.002 (h-j)	0.041 ± 0.002 (i-k)	5.93 ± 0.249 (a-c)	0.079 ± 0.004 (h-l)
V3, E 80%, 10 T	0.071 ± 0.002 (c-d)	0.069 ± 0.002 (d-e)	0.052 ± 0.001 (d-f)	7.76 ± 0.164 (b-f)	0.101 ± 0.003 (b-e)
V3, E 70%, 10 T	0.06 ± 0.002 (f-h)	0.058 ± 0.002 (g-i)	0.043 ± 0.001 (h-j)	6.09 ± 0.27 (b-e)	0.095 ± 0.003 (d-g)
V3, E 60%, 10 T	0.035 ± 0.003 (l-o)	0.033 ± 0.002 (n-q)	0.028 ± 0.001 (q-s)	4.37 ± 0.177 (a)	0.074 ± 0.005 (i-o)
V3, E 50%, 10 T	0.028 ± 0.002 (o-r)	0.026 ± 0.002 (r-t)	0.018 ± 0.001 (w-z)	2.93 ± 0.262 (a-b)	0.053 ± 0.003 (s-u)

Table 4. Impact of activated acacia wood biochar amendment on relative increase in leaf growth, and leaf area of three maize hybrids under varied moisture conditions. Note: The different letters in parenthesis after standard deviation represent significant variations among the treatments, as determined by the Tukey test and 95% confidence interval. Abbreviations: V1; DK-9108, V2; DK-6321, V3; Sarhaab, E; Evapotranspiration, T; tons biochar per hectare

Treatment	Membrane stability Index (%)		Malondialdehyde (nmol/ml)		Protein content (mg/g)	
	MSI Veg	MSI Rep	MDA Veg	MDA Rep	PC Veg	PC Rep
V1, 100% E, 0T	48.08 ± 2.52 (j-m)	38.08 ± 2.52 (lm)	4.34 ± 0.11 (c-e)	5.74 ± 0.22 (d-f)	4.35 ± 0.21 (n-q)	4.71 ± 0.21 (n-q)
V1, 80% E, 0T	33.07 ± 2.3 (op)	27.57 ± 2.3 (n-q)	4.87 ± 0.11 (c)	6.26 ± 0.22 (b-e)	3.83 ± 0.22 (p-w)	4.19 ± 0.25 (p-u)
V1, 70% E, 0T	27.31 ± 2.77 (p-r)	23.81 ± 1.77 (o-q)	5.61 ± 0.21 (b)	7.01 ± 0.21 (a-b)	3.23 ± 0.23 (u-y)	3.59 ± 0.23 (t-w)
V1, 60% E, 0T	23.05 ± 2.19 (qr)	20.05 ± 1.22 (q)	6.13 ± 0.12 (a-b)	7.53 ± 0.25 (a)	3.48 ± 0.28 (s-x)	3.93 ± 0.23 (r-v)
V1, 50% E, 0T	11.11 ± 2.14 (s)	11.87 ± 1.22 (r)	6.23 ± 0.13 (a)	7.63 ± 0.24 (a)	3.56 ± 0.24 (r-w)	3.84 ± 0.28 (s-v)
V1, 100% E, 5T	54.84 ± 1.24 (e-k)	40.12 ± 1.96 (j-m)	4.07 ± 0.31 (e)	5.47 ± 0.23 (e-f)	6.05 ± 0.24 (g-i)	6.43 ± 0.21 (g-i)
V1, 80% E, 5T	58.32 ± 1.77 (d-g)	50.65 ± 2.39 (d-g)	4.19 ± 0.13 (d-e)	5.59 ± 0.26 (d-f)	7.85 ± 0.21 (c-d)	8.23 ± 0.19 (c-e)
V1, 70% E, 5T	54.9 ± 1.4 (e-k)	47.5 ± 2.16 (e-j)	4.28 ± 0.11 (d-e)	5.68 ± 0.21 (d-f)	7.39 ± 0.24 (d-e)	7.74 ± 0.25 (de)
V1, 60% E, 5T	47.94 ± 1.77 (k-m)	41.74 ± 2.25 (i-m)	4.32 ± 0.21 (c-e)	6.03 ± 0.22 (c-f)	4.86 ± 0.2 (l-o)	5.21 ± 0.21 (l-o)
V1, 50% E, 5T	33.85 ± 2.28 (op)	28.55 ± 2.12 (no)	4.73 ± 0.21 (c-d)	6.37 ± 0.24 (b-d)	3.09 ± 0.22 (v-y)	3.44 ± 0.24 (u-w)
V1, 100% E, 10T	50.22 ± 2.75 (h-l)	39.22 ± 1.91 (lm)	4.05 ± 0.17 (e)	5.45 ± 0.24 (f)	5.45 ± 0.23 (i-l)	5.81 ± 0.23 (i-l)
V1, 80% E, 10T	57.6 ± 2.27 (e-h)	50.8 ± 2.27 (d-g)	4.35 ± 0.29 (c-e)	5.79 ± 0.25 (d-f)	6.13 ± 0.22 (g-i)	6.52 ± 0.19 (g-i)
V1, 70% E, 10T	53.92 ± 1.76 (e-k)	48.22 ± 1.76 (e-i)	4.44 ± 0.28 (c-e)	5.84 ± 0.25 (c-f)	6.13 ± 0.24 (g-i)	6.49 ± 0.23 (g-i)
V1, 60% E, 10T	41.97 ± 1.84 (mn)	37.77 ± 1.84 (lm)	4.58 ± 0.16 (c-e)	6.16 ± 0.23 (c-f)	4.01 ± 0.25 (p-t)	4.38 ± 0.25 (p-s)
V1, 50% E, 10T	26.98 ± 1.49 (p-r)	23.28 ± 2.34 (o-q)	4.84 ± 0.14 (c)	6.63 ± 0.21 (b-c)	3.09 ± 0.22 (w-y)	3.46 ± 0.24 (u-w)
V2, 100% E, 0T	55.35 ± 2.1 (e-k)	42.35 ± 2.9 (h-l)	1.68 ± 0.12 (i-l)	2.75 ± 0.22 (j-l)	5.39 ± 0.23 (i-l)	5.83 ± 0.25 (i-l)
V2, 80% E, 0T	43.5 ± 2.52 (lm)	39 ± 2.52 (lm)	1.89 ± 0.1 (i-l)	2.97 ± 0.24 (j-l)	5.13 ± 0.23 (k-m)	5.59 ± 0.22 (j-m)
V2, 70% E, 0T	30.82 ± 2.1 (op)	27.32 ± 2.1 (n-q)	2.06 ± 0.11 (i-j)	3.14 ± 0.23 (i-l)	5.05 ± 0.25 (l-n)	5.47 ± 0.24 (k-m)
V2, 60% E, 0T	31.18 ± 2.6 (op)	28.18 ± 2.6 (no)	2.16 ± 0.13 (h-i)	3.44 ± 0.26 (h-k)	2.71 ± 0.24 (x-y)	4.32 ± 0.24 (p-t)
V2, 50% E, 0T	28.14 ± 2.23 (o-r)	27.6 ± 2.23 (n-p)	3.37 ± 0.11 (f)	4.47 ± 0.25 (g)	3.87 ± 0.24 (p-v)	3.16 ± 0.25 (v-w)
V2, 100% E, 5T	61.23 ± 2.82 (c-e)	47.23 ± 1.82 (e-k)	0.48 ± 0.14 (r-s)	1.58 ± 0.26 (o)	7.05 ± 0.24 (e-f)	7.53 ± 0.25 (ef)
V2, 80% E, 5T	76.24 ± 2.19 (a)	69.57 ± 2.26 (a)	0.64 ± 0.18 (q-s)	1.74 ± 0.28 (o)	9.86 ± 0.22 (a)	10.36 ± 0.21 (a)
V2, 70% E, 5T	72.22 ± 1.61 (a-b)	64.82 ± 2.23 (a-b)	0.7 ± 0.11 (q-s)	1.82 ± 0.22 (n-o)	7.84 ± 0.22 (c-d)	8.32 ± 0.23 (cd)
V2, 60% E, 5T	55.54 ± 2.52 (e-j)	49.34 ± 2.52 (e-h)	0.74 ± 0.25 (q-s)	1.89 ± 0.3 (m-o)	5.89 ± 0.24 (g-k)	6.35 ± 0.24 (g-j)
V2, 50% E, 5T	52.61 ± 2.69 (f-k)	47.31 ± 2.69 (e-k)	0.97 ± 0.11 (o-r)	2.85 ± 0.24 (j-l)	3.36 ± 0.23 (t-x)	3.79 ± 0.22 (s-v)
V2, 100% E, 10T	57.71 ± 2.19 (e-g)	44.71 ± 2.19 (f-l)	0.41 ± 0.32 (s)	2.33 ± 0.23 (l-o)	5.92 ± 0.23 (g-j)	6.33 ± 0.22 (g-j)
V2, 80% E, 10T	65.78 ± 2.48 (b-d)	59.31 ± 2.56 (bc)	0.74 ± 0.1 (q-s)	2.59 ± 0.22 (l-n)	8.68 ± 0.23 (b)	9.11 ± 0.23 (b)
V2, 70% E, 10T	59.76 ± 2.51 (c-f)	54.06 ± 2.51 (c-e)	0.86 ± 0.08 (p-s)	2.78 ± 0.24 (j-l)	6.49 ± 0.22 (f-g)	6.95 ± 0.22 (fg)
V2, 60% E, 10T	53.03 ± 1.83 (f-k)	48.83 ± 2.83 (e-i)	1.06 ± 0.17 (n-q)	2.79 ± 0.24 (j-l)	4.37 ± 0.24 (m-p)	4.84 ± 0.24 (m-p)
V2, 50% E, 10T	43.76 ± 2.34 (lm)	40.06 ± 2.34 (j-m)	1.12 ± 0.1 (m-q)	3.11 ± 0.26 (i-l)	3.92 ± 0.22 (p-u)	4.41 ± 0.22 (p-s)
V3, 100% E, 0T	51.63 ± 2.18 (g-k)	39.63 ± 2.18 (lm)	2.65 ± 0.14 (g-h)	3.88 ± 0.35 (g-i)	5.17 ± 0.24 (j-l)	5.58 ± 0.24 (j-m)
V3, 80% E, 0T	35.03 ± 2.78 (no)	34.53 ± 2.78 (mn)	2.7 ± 0.15 (g-h)	3.92 ± 0.23 (g-i)	4.89 ± 0.23 (l-o)	5.31 ± 0.23 (k-o)
V3, 70% E, 0T	30.22 ± 1.7 (o-q)	26.72 ± 2.69 (o-q)	2.99 ± 0.14 (f-g)	4.2 ± 0.22 (g-h)	4.25 ± 0.24 (o-s)	4.64 ± 0.25 (o-r)
V3, 60% E, 0T	27.45 ± 1.98 (p-r)	24.45 ± 1.5 (o-q)	3.11 ± 0.12 (f-g)	4.4 ± 0.24 (g)	3.69 ± 0.24 (p-w)	4.09 ± 0.23 (p-u)
V3, 50% E, 0T	21.08 ± 2.33 (r)	20.54 ± 1.4 (pq)	4.39 ± 0.1 (c-e)	5.6 ± 0.21 (d-f)	2.56 ± 0.22 (y)	2.99 ± 0.23 (w)
V3, 100% E, 5T	57.58 ± 2.35 (e-h)	43.58 ± 2.35 (g-l)	1.42 ± 0.11 (k-o)	2.64 ± 0.4 (k-m)	6.33 ± 0.25 (f-h)	6.75 ± 0.25 (g-h)
V3, 80% E, 5T	66.79 ± 2.11 (bc)	57.89 ± 2.11 (b-d)	1.56 ± 0.17 (j-n)	2.78 ± 0.29 (j-l)	8.25 ± 0.23 (b-c)	8.66 ± 0.23 (bc)
V3, 70% E, 5T	60.05 ± 2.71 (c-f)	52.65 ± 2.71 (c-e)	1.63 ± 0.13 (i-m)	2.86 ± 0.2 (j-l)	7.53 ± 0.21 (c-e)	7.92 ± 0.22 (c-e)
V3, 60% E, 5T	49.89 ± 1.27 (i-l)	43.69 ± 1.27 (g-l)	1.67 ± 0.19 (i-m)	3.11 ± 0.22 (i-l)	4.91 ± 0.22 (l-o)	5.31 ± 0.22 (k-o)
V3, 50% E, 5T	43.01 ± 2.48 (lm)	37.71 ± 2.48 (lm)	2.05 ± 0.19 (i-j)	3.53 ± 0.24 (h-j)	3.21 ± 0.24 (u-y)	3.64 ± 0.24 (s-w)
V3, 100% E, 10T	53.77 ± 2.83 (e-k)	42.77 ± 2.83 (h-l)	1.34 ± 0.11 (l-p)	2.56 ± 0.23 (l-n)	5.63 ± 0.24 (h-l)	6.02 ± 0.24 (h-k)
V3, 80% E, 10T	60.56 ± 2.64 (c-e)	53.76 ± 2.64 (c-e)	1.69 ± 0.11 (i-l)	2.91 ± 0.24 (j-l)	7.45 ± 0.24 (d-e)	7.87 ± 0.24 (de)
V3, 70% E, 10T	57.02 ± 2.29 (e-i)	51.32 ± 2.29 (d-f)	1.79 ± 0.19 (i-l)	3.02 ± 0.22 (j-l)	6.28 ± 0.24 (f-h)	6.71 ± 0.24 (g-h)
V3, 60% E, 10T	44.04 ± 2.28 (lm)	39.84 ± 2.28 (k-m)	1.97 ± 0.18 (i-k)	3.42 ± 0.21 (h-k)	4.31 ± 0.25 (n-r)	4.73 ± 0.25 (n-q)
V3, 50% E, 10T	28.17 ± 1.98 (o-r)	24.47 ± 1.98 (o-q)	2.15 ± 0.13 (h-i)	4.17 ± 0.22 (g-h)	3.59 ± 0.23 (q-w)	3.98 ± 0.24 (q-u)

Table 5. Impact of activated acacia wood biochar amendment on membrane stability index, malondialdehyde, and protein content of three maize hybrids under varied moisture conditions. Note: The different letters in parenthesis after standard deviation represent significant variations among the treatments, as determined by the Tukey test and 95% confidence interval. Abbreviations: V1; DK-9108, V2; DK-6321, V3; Sarhaab, E; Evapotranspiration, T; tons biochar per hectare

Treatment	Superoxidase dismutase (U/mg)		Peroxidase (U/mg)		Catalase (U/mg)	
	SOD Veg	SOD Rep	POD Veg	POD Rep	CAT Veg	CAT Rep
V1, 100% E, 0T	3.08 ± 0.49 (s)	30.67 ± 2.95 (z)	3.08 ± 0.49 (v)	4.72 ± 1.09 (s)	16.59 ± 1.19 (t)	36.52 ± 1.99 (w)
V1, 80% E, 0T	5.74 ± 0.81 (p-r)	35.92 ± 2.15 (w-z)	5.74 ± 0.81 (s-u)	7.33 ± 0.82 (p-s)	19.49 ± 1.07 (q-t)	42.28 ± 2.27 (v-w)
V1, 70% E, 0T	9.07 ± 0.86 (j-o)	50.65 ± 2.83 (r-u)	8.01 ± 0.91 (q-t)	8.91 ± 0.35 (m-q)	23.43 ± 1.52 (m-r)	54.35 ± 2.89 (p-u)
V1, 60% E, 0T	10.06 ± 0.83 (h-k)	63.2 ± 2.68 (n-q)	11.06 ± 1.1 (n-p)	18.92 ± 0.72 (e-g)	23.22 ± 1.2 (m-r)	67.12 ± 2.1 (k-m)
V1, 50% E, 0T	12.5 ± 0.95 (f-h)	90.09 ± 2.44 (h-j)	14.89 ± 0.89 (k-l)	22.1 ± 0.79 (d)	38.71 ± 1.08 (e-f)	85.32 ± 3.54 (g-i)
V1, 100% E, 5T	5.19 ± 0.34 (r-s)	33.57 ± 3.1 (x-z)	5.19 ± 0.67 (u-v)	6.54 ± 0.73 (q-s)	21.03 ± 1.12 (p-t)	55.3 ± 3.33 (p-u)
V1, 80% E, 5T	6.86 ± 0.84 (o-r)	42.39 ± 2.17 (u-x)	6.87 ± 0.49 (r-u)	10.73 ± 0.47 (j-n)	26.41 ± 1.3 (k-n)	62.93 ± 3.51 (l-o)
V1, 70% E, 5T	7.44 ± 0.64 (l-r)	59.26 ± 2.41 (o-r)	7.44 ± 0.58 (q-u)	12.3 ± 0.86 (h-k)	29.48 ± 1.76 (i-l)	68.01 ± 2.87 (k-l)
V1, 60% E, 5T	16.19 ± 0.96 (e)	90.45 ± 3.19 (g-k)	18.05 ± 0.64 (j)	20.81 ± 0.3 (d-e)	37.81 ± 1.33 (e-f)	81.59 ± 3.1 (h-j)
V1, 50% E, 5T	28.4 ± 1.11 (c)	101.34 ± 3.09 (d-f)	26.34 ± 0.73 (e-f)	26.05 ± 0.97 (c)	54.46 ± 1.51 (b)	115.73 ± 3.28 (c)
V1, 100% E, 10T	5.11 ± 0.88 (r-s)	31.19 ± 3.2 (z)	5.11 ± 0.53 (u-v)	5.08 ± 0.65 (s)	19.22 ± 1.8 (r-t)	48.74 ± 2.43 (u-v)
V1, 80% E, 10T	5.91 ± 0.59 (p-r)	40.5 ± 3.07 (v-y)	5.91 ± 0.78 (s-u)	6.47 ± 0.59 (q-s)	21.61 ± 1.41 (o-s)	52.5 ± 2.48 (r-u)
V1, 70% E, 10T	8.01 ± 1.01 (k-p)	54.34 ± 2.78 (q-s)	9.07 ± 0.92 (p-r)	6.83 ± 0.77 (q-s)	26.09 ± 1.00 (l-o)	59.05 ± 2.89 (m-s)
V1, 60% E, 10T	13.32 ± 0.7 (f-g)	79.75 ± 2.38 (k-l)	14.37 ± 0.83(k-m)	11.38 ± 0.91 (j-m)	32.55 ± 1.19 (g-j)	77.2 ± 3.14 (i-j)
V1, 50% E, 10T	22.68 ± 0.94 (d)	93.79 ± 2.79 (f-j)	22.45 ± 0.54 (g-h)	17.99 ± 0.94 (f-g)	48.84 ± 1.72 (c-d)	111.32 ± 3.08 (c-d)
V2, 100% E, 0T	6.2 ± 0.57 (p-r)	36.67 ± 3.25 (w-z)	6.18 ± 0.49 (s-u)	9.54 ± 0.8 (l-p)	21.05 ± 1.62 (p-t)	50.79 ± 2.78 (s-v)
V2, 80% E, 0T	7.2 ± 0.84 (m-r)	44.23 ± 2.93 (t-w)	7.2 ± 1.14 (q-u)	10.25 ± 0.29 (j-o)	29.08 ± 1.11 (i-l)	51.05 ± 2.64 (r-u)
V2, 70% E, 0T	9.35 ± 0.62 (j-n)	63.61 ± 3.24 (n-p)	11.51 ± 0.91 (n-p)	12.14 ± 0.49 (h-l)	33.12 ± 1.14 (g-i)	62.87 ± 3.08 (l-p)
V2, 60% E, 0T	14.69 ± 0.49 (e-f)	94.14 ± 3.63 (f-i)	24.31 ± 0.47 (f-g)	19.51 ± 0.72 (d-g)	35.92 ± 1.41 (e-g)	83.88 ± 2.74 (h-i)
V2, 50% E, 0T	20.59 ± 0.7 (d)	118.59 ± 2.46 (b-c)	24.69 ± 0.58 (f-g)	30.57 ± 0.63 (b)	55.32 ± 1.18 (b)	103.79 ± 2.7 (d-e)
V2, 100% E, 5T	6.9 ± 0.6 (n-r)	47.62 ± 2.51 (s-v)	6.9 ± 0.32 (r-u)	11.02 ± 0.55 (j-n)	29.12 ± 1.23 (i-l)	61.32 ± 3.17 (l-q)
V2, 80% E, 5T	7.92 ± 0.78 (k-q)	54.75 ± 2.27 (p-s)	7.92 ± 0.55 (q-t)	13.38 ± 0.96 (h-j)	36.4 ± 1.67 (e-g)	67.99 ± 3.11 (k-l)
V2, 70% E, 5T	11.51 ± 0.76 (g-j)	77.25 ± 3.17 (k-m)	9.35 ± 0.62 (p-r)	18.56 ± 0.59 (e-g)	36.35 ± 1.45 (e-g)	79.71 ± 3.13 (i-j)
V2, 60% E, 5T	26.92 ± 0.68 (c)	103.57 ± 3.28 (d-e)	28.59 ± 0.94 (d-e)	26.39 ± 0.65 (c)	47.3 ± 1.21 (d)	95.75 ± 2.9 (e-f)
V2, 50% E, 5T	38.58 ± 0.7 (a)	134.67 ± 2.86 (a)	34.8 ± 0.58 (a)	36.62 ± 1.07 (a)	63.13 ± 1.41 (a)	128.84 ± 3.11 (a)
V2, 100% E, 10T	7.36 ± 0.4 (l-r)	41.26 ± 3.00 (v-y)	7.36 ± 0.86 (q-u)	10.63 ± 0.7 (j-o)	22.04 ± 1.22 (n-r)	53.25 ± 2.95 (q-u)
V2, 80% E, 10T	7.45 ± 1.02 (l-r)	47.35 ± 1.98 (s-v)	7.45 ± 0.79 (q-u)	9.55 ± 1.09 (l-p)	27.58 ± 1.04 (k-m)	57.56 ± 2.6 (o-t)
V2, 70% E, 10T	12.08 ± 0.45 (g-i)	70.47 ± 2.29 (m-n)	12.09 ± 0.99(m-o)	11.58 ± 0.85 (i-l)	34.45 ± 0.94 (f-h)	66.31 ± 3.25 (k-n)
V2, 60% E, 10T	21.31 ± 0.62 (d)	99.37 ± 3.24 (d-g)	19.16 ± 0.94 (i-j)	17.28 ± 0.84 (g)	45.03 ± 1.3 (d)	90.14 ± 3.22 (f-h)
V2, 50% E, 10T	32.46 ± 0.67 (b)	126.74 ± 2.84 (a-b)	31.46 ± 0.55 (b-c)	25.13 ± 1.08 (c)	54.14 ± 1.59 (b)	118.1 ± 2.56 (b-c)
V3, 100% E, 0T	5.51 ± 0.53 (q-s)	44.91 ± 2.14 (t-w)	5.47 ± 0.93 (t-v)	6.25 ± 0.85 (r-s)	17.49 ± 1.02 (s-t)	48.5 ± 3.02 (u-v)
V3, 80% E, 0T	7.76 ± 0.82 (k-q)	51.75 ± 1.7 (r-t)	6.83 ± 0.82 (r-u)	8.09 ± 0.28 (o-r)	21.75 ± 1.85 (o-s)	50.85 ± 2.19 (s-v)
V3, 70% E, 0T	7.41 ± 0.34 (l-r)	68.69 ± 2.62 (m-n)	7.41 ± 0.76 (q-u)	10.85 ± 0.36 (j-n)	25.18 ± 1.11 (l-p)	55.68 ± 2.97 (p-u)
V3, 60% E, 0T	12.6 ± 0.59 (f-g)	95.64 ± 2.14 (e-i)	12.6 ± 0.59 (l-n)	20.3 ± 0.87 (d-f)	29.25 ± 1.82 (i-l)	73.12 ± 2.94 (j-k)
V3, 50% E, 0T	16.52 ± 0.64 (e)	117.29 ± 2.18 (c)	23.05 ± 0.93 (g-h)	26.95 ± 1.02 (c)	47.34 ± 1.73 (d)	97.29 ± 2.03 (e-f)
V3, 100% E, 5T	6.97 ± 0.68 (n-r)	33.1 ± 2.83 (y-z)	6.97 ± 1.09 (r-u)	8.87 ± 0.92 (m-r)	25.12 ± 1.11 (l-p)	59.48 ± 2.73 (l-r)
V3, 80% E, 5T	8.11 ± 0.66 (k-p)	42.74 ± 2.11 (t-w)	8.11 ± 1.05 (q-s)	11.21 ± 1.06 (j-n)	30.64 ± 0.95 (h-k)	64.36 ± 2.36 (l-o)
V3, 70% E, 5T	9.78 ± 0.85 (i-l)	57.26 ± 2.54 (o-r)	9.78 ± 0.85 (o-q)	14.3 ± 0.57 (h)	34.2 ± 1.63 (f-h)	73.28 ± 3.12 (j-k)
V3, 60% E, 5T	21.61 ± 0.64 (d)	84.99 ± 2.92 (j-l)	20.94 ± 1.04 (h-i)	21.61 ± 0.84 (d)	39.81 ± 1.16 (e)	93.58 ± 2.32 (f-g)
V3, 50% E, 5T	33.2 ± 1.06 (b)	98.85 ± 2.62 (d-h)	32.1 ± 0.62 (b)	31.83 ± 0.65 (b)	62.86 ± 1.28 (a)	124.94 ± 3.17 (a-b)
V3, 100% E, 10T	6.35 ± 0.37 (p-r)	36 ± 1.95 (w-z)	6.35 ± 0.65 (s-u)	4.93 ± 0.93 (s)	20.43 ± 1.26 (q-t)	50.34 ± 1.73 (t-v)
V3, 80% E, 10T	6.87 ± 0.58 (o-r)	46.46 ± 2.93 (s-v)	7.97 ± 0.48 (q-t)	6.6 ± 1.06 (q-s)	23.81 ± 1.35 (m-q)	54.07 ± 3.11 (q-u)
V3, 70% E, 10T	9.54 ± 0.5 (j-m)	63.86 ± 3.21 (n-o)	9.33 ± 0.79 (p-r)	8.64 ± 0.74 (n-r)	28.35 ± 0.82 (j-l)	58.45 ± 2.33 (n-t)
V3, 60% E, 10T	16.8 ± 0.71 (e)	88.53 ± 2.44 (i-k)	16.94 ± 0.81 (j-k)	14.07 ± 1.05 (h-i)	36.55 ± 1.44 (e-g)	80.63 ± 2.64 (i-j)
V3, 50% E, 10T	26.52 ± 1.03 (c)	106.86 ± 2.28 (d)	29.21 ± 1.09 (c-d)	20.63 ± 0.42 (d-e)	52.72 ± 1.55 (b-c)	114.68 ± 3.25 (c)

Table 6. Impact of activated acacia wood biochar amendment on antioxidant enzymes (SOD, POD, and CAT) assay of three maize hybrids under varied moisture conditions. Note: The different letters in parenthesis after standard deviation represent significant variations among the treatments, as determined by the Tukey test and 95% confidence interval. Abbreviations: V1; DK-9108, V2; DK-6321, V3; Sarhaab, E; Evapotranspiration, T; tons biochar per hectare

Yield analysis

The three-way ANOVA of maize hybrids, biochar supplementation levels, and moisture regimes revealed significant effects on thousand seed weight and total seed weight (Fig. 5). Reduced water availability led to a decrease in both 1000-seed weight and total seed weight of the maize hybrids. However, the application of biochar mitigated these reductions, significantly enhancing seed weights. Specifically, soil amended with 5 tons/ha of biochar increased the 1000-seed weight by 16% and total seed weight by 29% compared to non-amended soil. Moreover, treatments at 80% ETC resulted in higher seed weights than at 100%, 70%, 60%, and 50% ETC. The 1000-seed weight increased by 1.04, 1.05, 1.42, and 1.73 times, respectively, while the total seed weight improved by 1.07, 1.08, 1.46, and 1.98 times compared to the other ETC levels.

Water deficit conditions also resulted in reduced grain and stover yields of maize hybrids. However, biochar supplementation significantly improved these yields (Fig. 6). Soil amended with 5 tons/ha of biochar elevated grain yield and stover yield by 26% compared to non-amended soil. The 80% ETC treatments showed superior yields over 100%, 70%, 60%, and 50% ETC. Grain yield increased by 1.13, 1.10, 1.42, and 1.90 times, while stover yield improved by 1.02, 1.08, 1.38, and 1.68 times, respectively, compared to other ETC treatments.

The apparent water productivity (AWP) declined significantly under deficit irrigation (Fig. 7). However, the incorporation of biochar greatly enhanced AWP in maize hybrids. Soil amended with 5 tons/ha of biochar led to a 33% increase in AWP compared to non-amended soil. Interestingly, 70% ETC resulted in the highest AWP, surpassing 100%, 80%, 60%, and 50% ETC by 1.50, 1.18, 1.08, and 1.05 times, respectively.

Principal component analysis (PCA) and heatmap

The PCA biplot (Fig. 8) shows the first two principal components (PC1 and PC2), explaining 70.28% and 20.56% of the variance, respectively. The arrows indicate each variable's contribution to the principal components. Variables pointing in the same direction (e.g., membrane stability index, growth rate, weights, net assimilation rate, yield parameters) are positively correlated and mainly contribute to PC1. Variables in opposite directions (e.g., malondialdehyde content, stress indicators) are negatively correlated. The arrow length shows the variable's contribution strength. Ellipses represent 95% confidence intervals for treatment groups, highlighting variability. The red ellipse (0 t/ha Biochar) is distinct from the blue (10 t/ha Biochar) and green (5 t/ha Biochar) ellipses, indicating treatment differences. Higher Biochar treatments (5 t/ha and 10 t/ha) cluster together, separate from 0 t/ha, showing significant treatment effects. Different point shapes (triangles, squares, circles) denote the impact of ETC and variety on principal components, with clustering within ellipses suggesting intertwined effects with biochar treatments.

The heatmap (Fig. 9) shows the relationships between treatments and various biochemical, physiological, and yield parameters for maize. Darker colors (black/purple) indicate lower values, while lighter colors (yellow) indicate higher values. The combination of 5 t/ha biochar and 80% ETC yields the highest values across most parameters, suggesting it is the most favorable treatment. Water stress (50% ETC) significantly reduces growth and yield but increases stress-related biochemical responses. Different maize varieties respond uniquely to moisture and biochar levels, with DK-6321 showing the best tolerance to water stress, followed by SARHAAB and DK-9108.

Discussion

Soil physicochemical properties

This study yielded significant findings regarding the effects of biochar on several key soil physicochemical properties, including bulk density, particle density, total porosity, electrical conductivity, pH, organic carbon, organic matter, oxidizable carbon, phosphorus, and potassium levels. The most notable improvements were evident in soils amended with activated biochar compared to non-amended soils. However, the slight increase in electrical conductivity and pH observed in biochar-treated soil may be due to the salts present in biochar's ash content, consistent with findings by Liang et al.[55] and Saeed et al.[56]. While an increase in pH can be beneficial for nutrient availability in acidic soils, the long-term effects of increased electrical conductivity warrant further investigation to avoid potential salinity issues.

Biochar's influence on soil microbial activity is one of the key mechanisms driving these changes. Biochar creates a conducive environment for microbial colonization by providing a porous habitat that enhances microbial activity, thereby promoting the decomposition of organic residues and influencing the turnover of soil organic matter[57]. This microbial stimulation plays a vital role in nutrient cycling, increasing the availability of essential nutrients like nitrogen, phosphorus, and potassium. Furthermore, biochar's impact on soil properties, such as improved water infiltration and reduced runoff, can lead to an increased saturation percentage[58], thus improving water availability for crops, particularly in water-limited environments.

The observed increase in organic carbon and oxidizable carbon content signifies a positive impact on soil health and fertility. Organic carbon plays a crucial role in nutrient retention, water-holding capacity, and overall soil structure. Biochar's ability to act as a stable organic carbon pool helps sequester carbon in the soil, thereby influencing carbon dynamics[59,60]. This finding underscore biochar's potential role not only in improving soil fertility but also in contributing to climate change mitigation by serving as a long-term carbon sink.

In addition, biochar's enhancement of nutrient levels, including nitrogen, phosphorus, and potassium, can be attributed to its high cation exchange capacity (CEC), which allows it to retain and release nutrients more efficiently[61]. By increasing the CEC of soil particles, biochar ensures that essential nutrients remain available for plant uptake, which is especially beneficial in soils with low fertility.

SEM-EDX analysis revealed that the major elements in the soil were carbon, oxygen, magnesium, silicon, potassium, calcium, aluminum, and iron, with trace amounts of sodium and titanium. This elemental composition aligns with the typical mineral content of soils dominated by silicate minerals like feldspar and quartz[62]. The presence of high Si and O concentrations in silica particles (SiO_2) indicates the significant quartz content, which

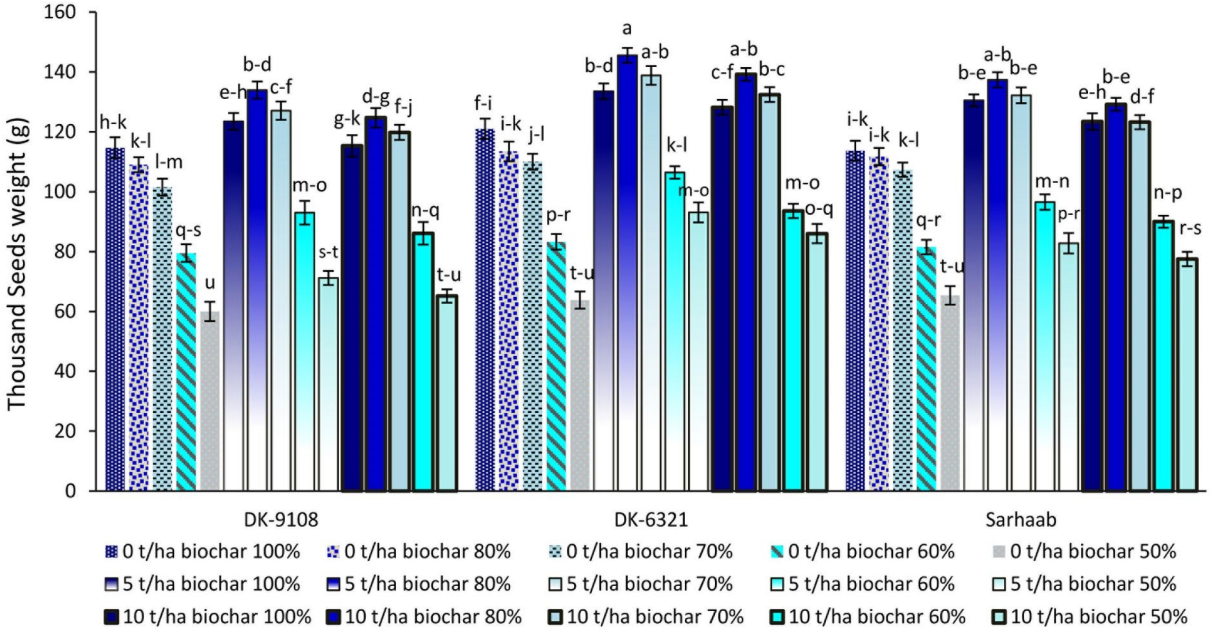

(b)

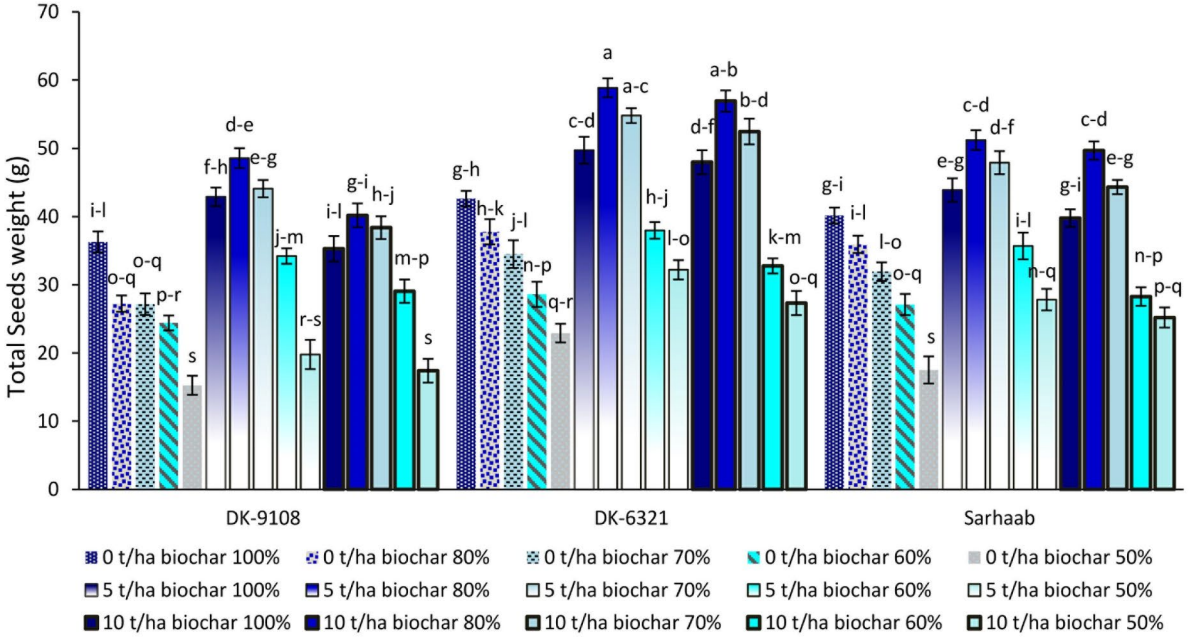

Fig. 5. Impact of activated acacia biochar amendment on (**a**) thousand seed weight and (**b**) total seed weight in maize hybrids under varied moisture conditions. Note: Different letters on bars represent significant variations among the treatments, as determined by Tukey Pairwise Comparison of ETC × Amendment × Variety at 95% confidence interval.

constitutes nearly 50% of the soil's mineral makeup[63]. Additionally, the presence of alkali feldspars, particularly potassium and sodium, highlights the soil's mineralogical diversity.

The carbon content detected in all samples, including those from non-amended soils, is likely due to peat formation[64]. However, the highest carbon content observed in soils supplemented with 10 tons/ha of biochar

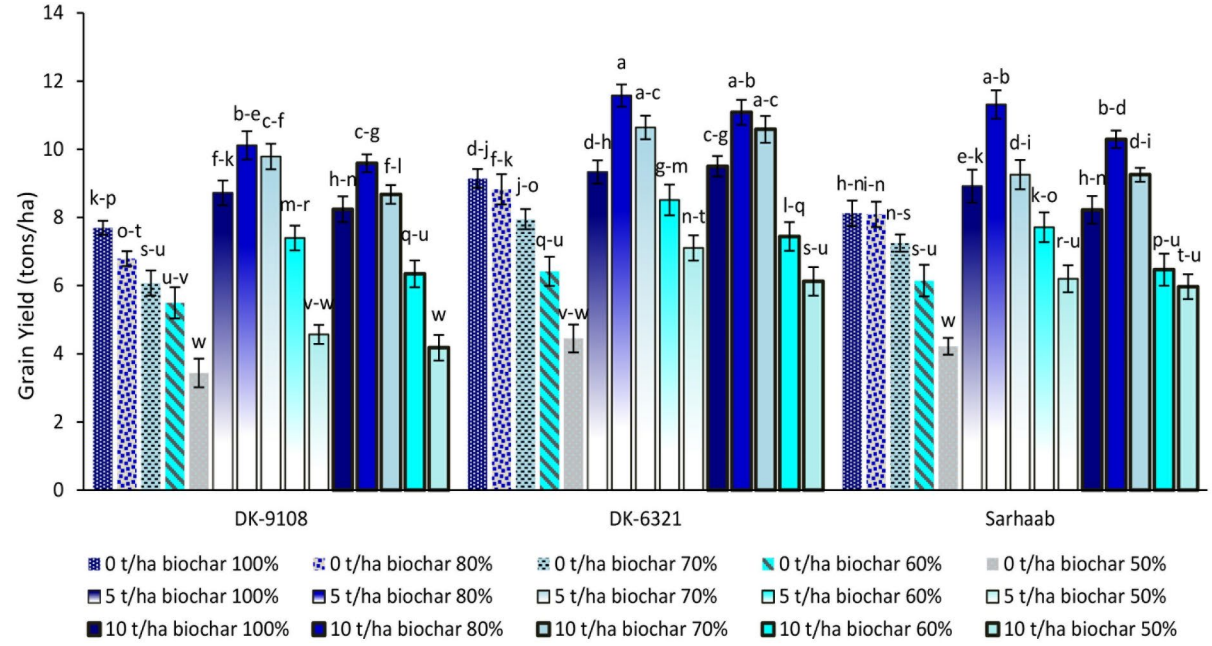

(b)

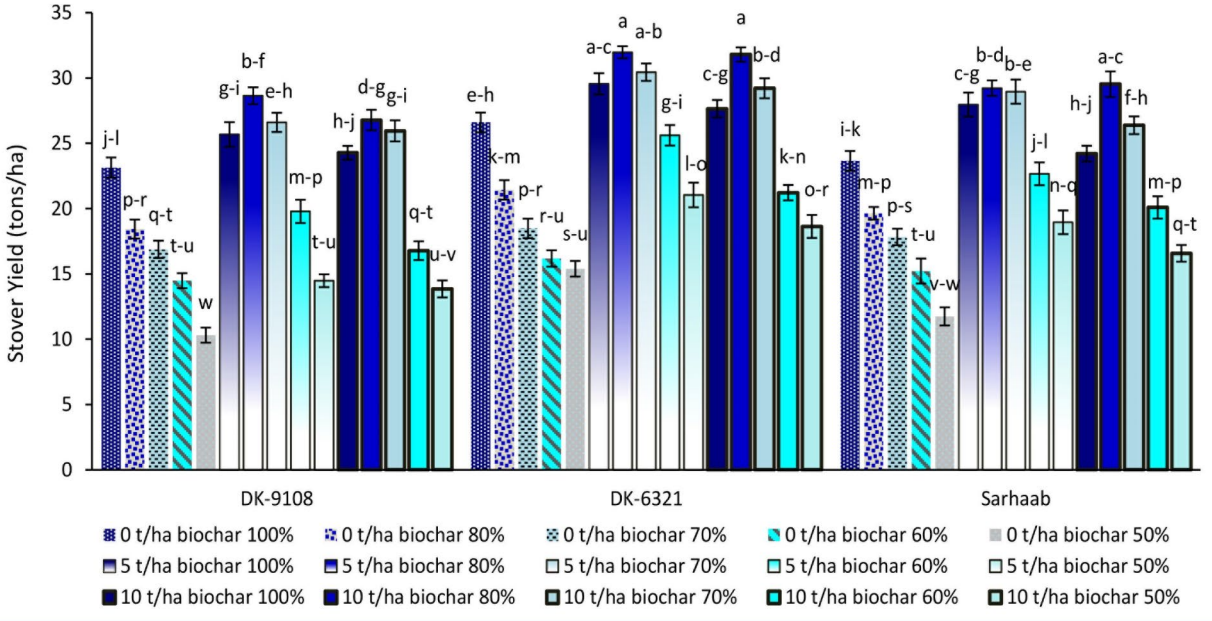

Fig. 6. Impact of activated acacia biochar amendment on (**a**) grain yield and (**b**) stover yield in maize hybrids under varied moisture conditions. Note: Different letters on bars represent significant variations among the treatments, as determined by Tukey Pairwise Comparison of ETC × Amendment × Variety at 95% confidence interval.

can be attributed to the recalcitrant carbon added by biochar[65]. This recalcitrant carbon is more resistant to decomposition and thus contributes to long-term carbon storage in the soil.

Moreover, biochar's ability to improve soil structure is well-established. By enhancing soil aggregation, biochar increases the soil's water retention capacity[66], which is particularly beneficial in arid and semi-arid regions.

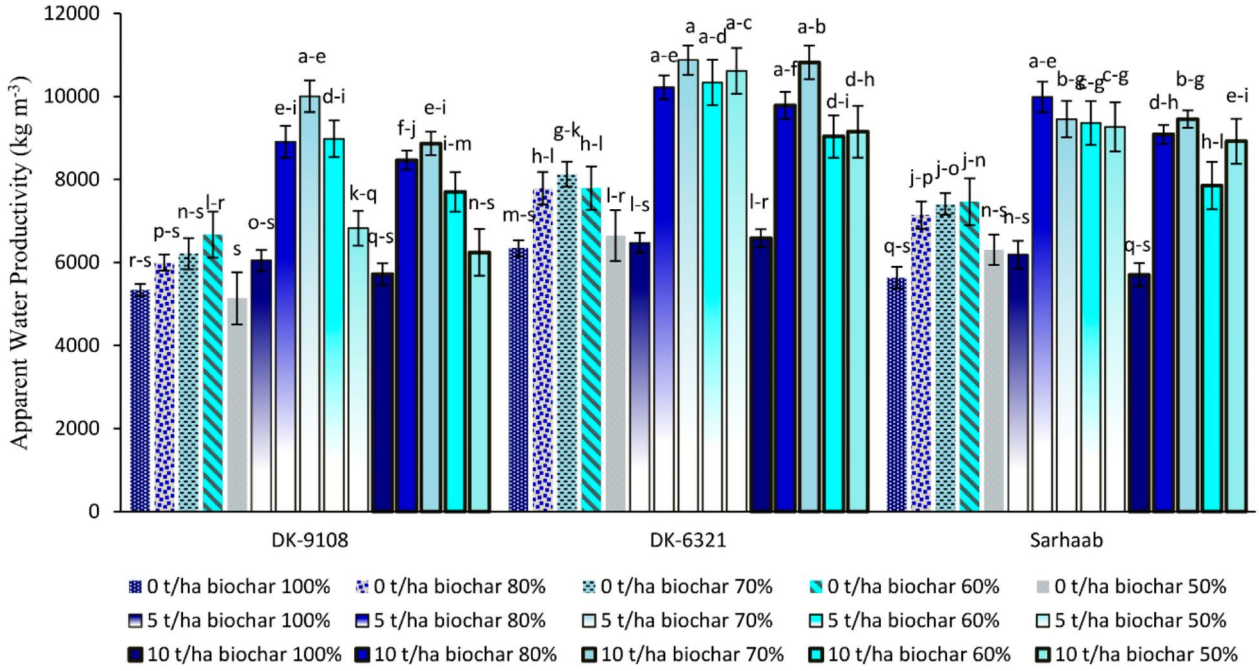

Fig. 7. Impact of activated acacia biochar amendment on apparent water productivity in maize hybrids under varied moisture conditions. Note: Different letters on bars represent significant variations among the treatments, as determined by Tukey Pairwise Comparison of ETC × Amendment × Variety at 95% confidence interval.

However, the presence of fine particles in biochar may reduce the saturated hydraulic conductivity of soils[67], indicating the need for careful selection of biochar types and application rates to avoid any negative impact on soil water movement. Biochar's porous structure improves soil aeration and reduces compaction, promoting better root growth. Enhanced root development allows plants to access water and nutrients more effectively, especially in drought-prone soils. The improvement in root biomass leads to better nutrient uptake, contributing to higher crop yields[69–71]. Increased microbial activity in biochar-amended soils plays a crucial role in nutrient cycling. Biochar offers a protective environment for beneficial soil microorganisms, such as nitrogen-fixing and phosphorus-solubilizing bacteria, which improve nutrient availability. This microbial enhancement can also lead to better decomposition of organic matter, releasing more nutrients into the soil [72–74]. Biochar's high surface area and cation exchange capacity (CEC) allow it to adsorb and retain nutrients like nitrogen, phosphorus, and potassium. The study's findings of increased phosphorus and potassium levels in biochar-amended soils suggest biochar actively enhances nutrient availability while reducing leaching losses. This leads to sustained fertility over time and reduces the need for synthetic fertilizers [75,76].

Influence of biochar supplementation on maize growth

Abiotic stress significantly reduces plant growth by disrupting physiological processes leading to lower the plant growth[76]. Insufficient water availability leads to a notable reduction in root and shoot biomass, as well as a comparative decline in growth rates in plants. This reduction can be attributed to multiple factors, including limited water uptake due to reduced soil moisture accessibility, oxidative stress-induced root and shoot cell damage, the reallocation of resources to prioritize critical survival functions over root and shoot development, and impaired nutrient absorption[77]. Additionally, water stress inhibits cellular expansion and division, which further limits plant growth[78].

Conversely, the application of biochar into the soil significantly improved root and shoot dry and fresh weight under water stress conditions. This improvement can be explained by several key factors. Biochar's porous structure enhances soil moisture retention by acting as a sponge, which increases water availability to plant roots even during periods of water deficit[79]. Moreover, biochar's ability to improve the soil's cation exchange capacity (CEC) helps increase nutrient availability, ensuring a steady supply of essential nutrients such as nitrogen, phosphorus, and potassium to the plants[80]. These nutrients are critical for root and shoot growth, particularly under stress conditions. Additionally, biochar's positive influence on soil structure reduces compaction and provides a more aerated environment, supporting healthier root development[81].

Biochar also helps to mitigate oxidative stress by reducing the accumulation of reactive oxygen species (ROS), which are responsible for cellular damage in plant tissues during drought[82]. Furthermore, biochar fosters the growth of beneficial soil microbial communities, including symbiotic fungi like arbuscular mycorrhizal fungi (AMF), which can help plants access nutrients more effectively, particularly under water-limited conditions[83].

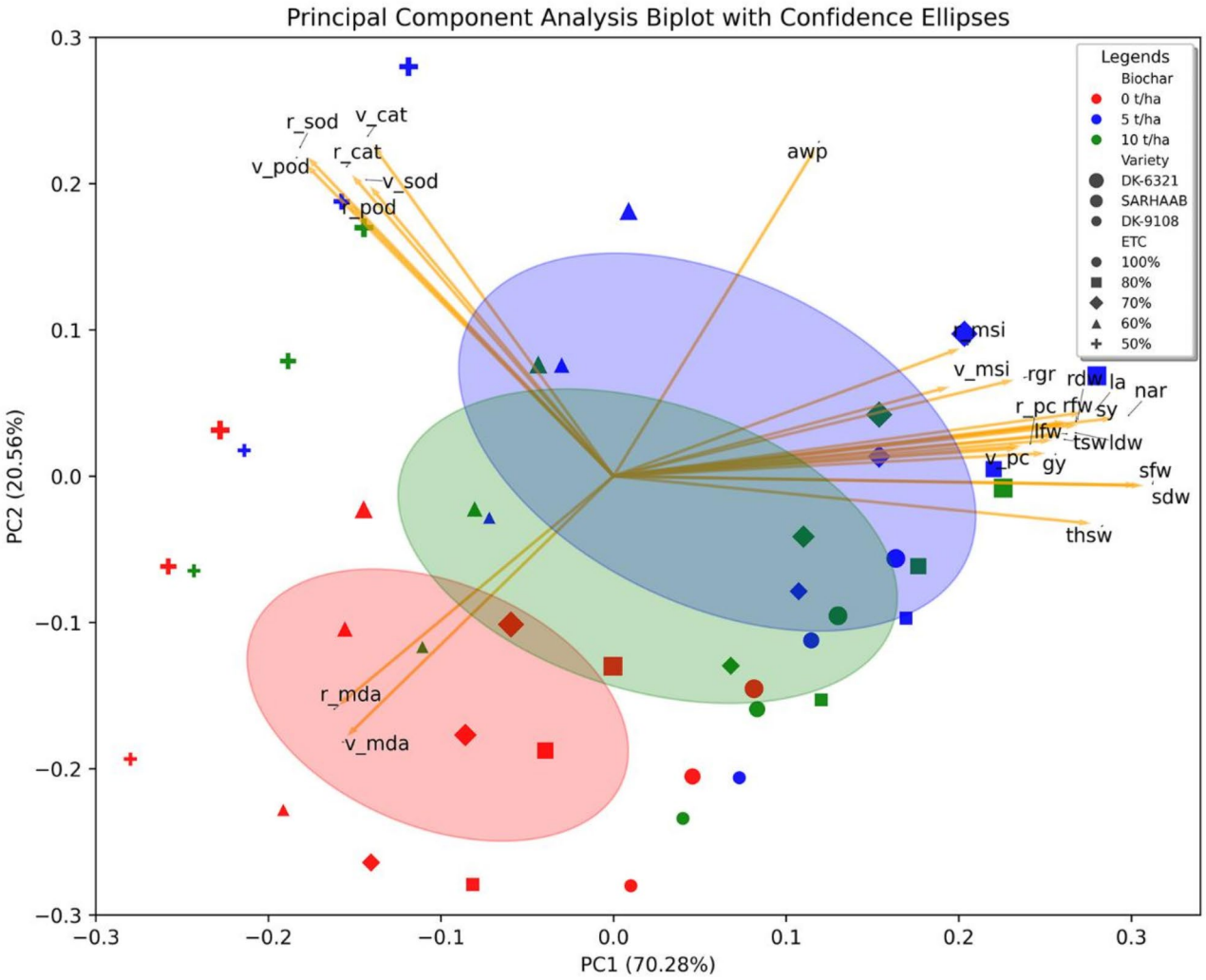

Fig. 8. Biplot of principal component analysis showing the various physiological and biochemical attributes of maize hybrids grown in biochar amended and non-amended soil under different moisture levels of ETC. Abbreviations: rfw: root fresh weight, rdw: root dry weight, sfw: shoot fresh weight, sdw: shoot dry weight, lfw: leaf fresh weight, ldw: leaf dry weight, la: leaf area, nar: net assimilation rate, rgr: relative growth rate, v_msi: vegetative membrane stability, r_msi: reproductive membrane stability, v_mda: vegetative malondialdehyde content, r_mda: reproductive malondialdehyde content, v_pc: vegetative protein content, r_pc: reproductive protein content, v_sod: vegetative superoxidase dismutase activity, r_sod: reproductive superoxidase dismutase activity, v_pod: vegetative peroxidase activity, r_pod: reproductive peroxidase activity, v_cat: vegetative catalase activity, r_cat: reproductive catalase activity, tsw: total seeds weight, thsw: thousand seed weight, gy: grain yield, sy: stover yield, awp: apparent water productivity.

These mutual benefits create a more conducive environment for roots to access water and nutrients and for shoots to maintain photosynthesis and growth. As a result, biochar application leads to increased root and shoot biomass, even when facing water stress challenges.

Water stress typically causes a decline in leaf live and dehydrated mass weight, as well as a reduction in leaf area. These effects result from the plant's limited ability to maintain turgor pressure, which is crucial for cell expansion and overall leaf growth. Additionally, water stress can induce oxidative stress in leaves, damaging their cellular structure and further hindering growth[84]. Reduced leaf area compromises the plant's capacity to capture sunlight and carry out efficient photosynthesis, leading to lower growth rates.

However, when biochar is applied to the soil, it has been shown to mitigate these negative effects. Studies indicate that biochar application results in increased leaf live and dehydrated mass weight, as well as an expansion of leaf area, even under water stress conditions[85]. This improvement is due to biochar's ability to retain soil moisture and improve the availability of essential nutrients like nitrogen and potassium, which are critical for leaf development[86]. Additionally, biochar has been shown to reduce the impact of oxidative stress on leaf cells, promoting healthier and more vigorous leaves[87]. By improving both water and nutrient availability, biochar ultimately enhances leaf growth and biomass, allowing the plant to maintain larger leaf areas under water-restricted conditions.

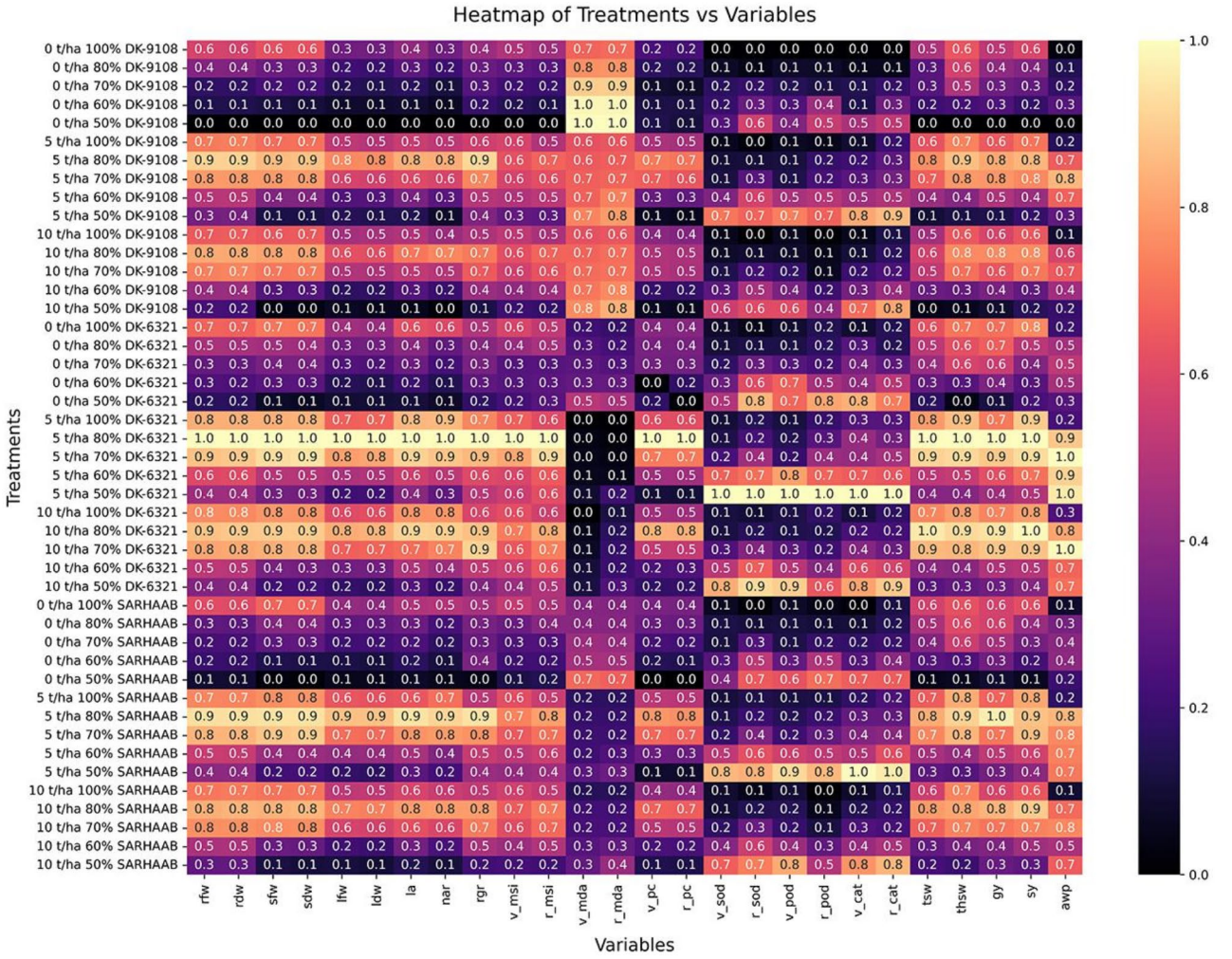

Fig. 9. Heatmap showing the relation of maize hybrids, biochar amendments and plants growth attributes at vegetative, reproductive and maturity stages. Abbreviations: rfw: root fresh weight, rdw: root dry weight, sfw: shoot fresh weight, sdw: shoot dry weight, lfw: leaf fresh weight, ldw: leaf dry weight, la: leaf area, nar: net assimilation rate, rgr: relative growth rate, v_msi: vegetative membrane stability, r_msi: reproductive membrane stability, v_mda: vegetative malondialdehyde content, r_mda: reproductive malondialdehyde content, v_pc: vegetative protein content, r_pc: reproductive protein content, v_sod: vegetative superoxidase dismutase activity, r_sod: reproductive superoxidase dismutase activity, v_pod: vegetative peroxidase activity, r_pod: reproductive peroxidase activity, v_cat: vegetative catalase activity, r_cat: reproductive catalase activity, tsw: total seeds weight, thsw: thousand seed weight, gy: grain yield, sy: stover yield, awp: apparent water productivity.

Water stress also leads to a decline in the net assimilation rate (NAR) of plants, as the limited availability of water restricts stomatal opening, thereby reducing CO2 intake and hindering the photosynthesis process[88]. As a result, carbon assimilation is reduced, leading to lower biomass production and consequently a decline in NAR[89]. In drought conditions, photosynthesis is further impaired by the overproduction of ROS, which damages the photosynthetic machinery and reduces the plant's ability to fix carbon[90].

However, biochar application has been found to significantly boost NAR under water stress conditions. This enhancement is largely driven by biochar's ability to improve soil water retention, which alleviates drought-induced limitations on photosynthesis[91]. Moreover, biochar promotes nutrient availability, particularly nitrogen, which is a critical component of chlorophyll and plays a central role in photosynthesis[92]. By creating favorable conditions for leaf development and reducing oxidative stress, biochar enables plants to maintain higher rates of carbon assimilation, thereby increasing NAR even under hydric stress. Furthermore, biochar-induced improvements in stomatal regulation help to optimize gas exchange and maintain photosynthetic efficiency during drought conditions[93].

Influence on physiological, biochemical, and yield attributes

Water stress typically leads to an increase in oxidative stress within plant cells, which can result in membrane damage and instability due to lipid peroxidation. This finding that a reduction in the Membrane Stability Index

(MSI) of dehydrated plants, as reactive oxygen species (ROS) accumulate and disrupt cellular functions is consistent with the reports[94]. When plants face limited water availability, the imbalance of ROS can damage cell membranes, disrupting ion transport, and leading to cell dehydration. In contrast, biochar-amended soil offers a more favorable growing environment under these stress conditions. Biochar's water-retentive properties and ability to improve nutrient availability play a critical role in maintaining cell turgor pressure and reducing oxidative stress, as the outcomes mirrored by the insight[95]. Enhanced soil aeration and a balanced nutrient profile help plants maintain structural integrity even during periods of hydric stress. This explains why plants grown in biochar-amended soil exhibit higher MSI values, even under drought conditions, compared to non-amended counterparts. Furthermore, biochar improving the plant's ability to cope with water scarcity by mitigating the stress experienced during the reproductive stage, where plants generally exhibit lower MSI values than during the vegetative phase due to the heightened sensitivity to water stress during reproduction, is echoed by the finding[96].

The abiotic stress also stimulates oxidative damage in plants, leading to an accumulation of malondialdehyde (MDA), a marker of lipid peroxidation and cellular injury, as reported[97,98]. Elevated MDA levels are an indicator of severe oxidative stress in plant tissues, often resulting in compromised physiological processes. However, the application of biochar significantly alleviated the impact of water stress on MDA accumulation by enhancing soil water retention, thereby reducing the severity of the drought stress experienced by plants, in parallel to the finding[99]. Additionally, biochar fosters a favorable rhizosphere environment by promoting beneficial microbial communities and improving nutrient availability, which together strengthen the plant's resilience to oxidative damage[100]. Consequently, biochar-treated plants tend to exhibit lower MDA levels compared to untreated plants under similar conditions, highlighting biochar's role in reducing oxidative stress. Moreover, it is well-documented that plants in the reproductive stage tend to accumulate more MDA compared to the vegetative stage, which reflects the increased vulnerability of reproductive tissues to water stress[101]. This reduction in oxidative damage underscores biochar's potential as a soil amendment that enhances plant health and tolerance to environmental challenges.

Protein content is another critical biochemical attribute negatively affected by water stress. Under drought conditions, plants often exhibit a reduction in protein content, primarily due to a slowdown in metabolic processes such as protein synthesis[102]. The hydration-deficiency caused by water stress limits the ability of plants to perform essential cellular functions, resulting in lower protein production. This reduction compromises a plant's capacity to respond to stress and maintain physiological activity. However, biochar application has shown promising results in mitigating the decline in protein content. Biochar-enhanced soils provided better water retention and nutrient availability, enabling plants to maintain metabolic processes, including protein synthesis, under limited moisture conditions, as reported[103]. As a result, plants grown in biochar-amended soils exhibit higher protein levels compared to those in non-amended soils, even under drought stress. Furthermore, protein content often peaks during the reproductive stage due to stress-induced expression of proteins involved in protecting plants from environmental stresses, similar to the reports [104,105]. This demonstrates biochar's role in maintaining protein levels and sustaining plant metabolism during critical growth stages.

Water stress also induces a heightened production of antioxidant enzymes such as superoxide dismutase (SOD), peroxidase (POD), and catalase (CAT). These enzymes are key components of the plant's defense system against oxidative stress caused by ROS overproduction[106]. Under drought conditions, these antioxidant enzymes help scavenge excess ROS, mitigating potential damage to cellular structures. However, the addition of biochar into the soil moderated the impact of water stress on antioxidant enzyme activity by improving soil water retention and reducing the need for extensive ROS scavenging, in mirror to the finding[107]. As a result, biochar-treated plants exhibit a more balanced ROS-detoxifying enzyme profile. Not only does biochar directly enhance soil conditions, but it also indirectly affects enzyme activity by improving nutrient availability and fostering microbial communities[108]. The activity of these enzymes fluctuates between plant growth stages, with peroxidase and catalase levels tending to increase during the reproductive stage, while SOD activity decreases, finding showing similarity to reports [109,110]. This differential enzyme activity across growth stages further highlights biochar's ability to support plants under stress by influencing the antioxidant defense system.

In terms of yield, water stress exerts a detrimental effect on several yield components, including cob length, cob weight, kernel number, grain yield per hectare, stover yield, and apparent water productivity[111]. The reduction in soil moisture interferes with critical physiological processes, such as photosynthesis and nutrient translocation, resulting in lower crop productivity. However, biochar application has been shown to mitigate these yield losses by improving soil moisture retention, enhancing nutrient availability, and promoting beneficial microbial interactions[112]. Biochar's ability to enhance soil structure also creates a more favorable environment for root growth and nutrient uptake, contributing to better crop performance even under suboptimal water conditions.

Interestingly, the study observed that biochar application at a dosage of 5 tons/ha resulted in better physiological, biochemical, and yield outcomes than a higher dosage of 10 tons/ha. This suggests the possibility of diminishing returns with excessive biochar use, likely due to nutrient imbalances, such as nitrogen uptake limitation at higher biochar doses[113]. The optimal biochar dosage appears to strike a balance between promoting plant responses and avoiding nutrient saturation, underscoring the importance of fine-tuning biochar application rates in agricultural practices. This fine-tuning ensures that the benefits of biochar are maximized without causing adverse effects, thus highlighting biochar's potential as a sustainable tool for improving plant resilience and productivity under water stress conditions.

The findings of this study have significant implications for agriculture and environmental sustainability. Biochar's ability to improve soil structure, nutrient retention, and water-holding capacity makes it a valuable tool for enhancing crop productivity, particularly in regions with poor soil fertility or limited water resources

[114,115]. Its potential to sequester carbon also positions biochar as a viable strategy for mitigating climate change, as it can lock atmospheric carbon dioxide in stable soil carbon pools for extended periods[116].

Additionally, biochar can reduce the need for chemical fertilizers by enhancing the availability of essential nutrients, promoting more sustainable agricultural practices. This reduction in fertilizer use can lower input costs for farmers while minimizing the environmental impact associated with excessive fertilizer application, such as nutrient runoff and water pollution[117].

Conclusion

In conclusion, this study demonstrates the effectiveness of organically activated biochar in improving maize growth, biochemical, physiological traits, and yield under both optimal and water-deficit conditions. The research provides scientifically valuable insights into the potential of biochar as a soil amendment, particularly under field conditions where drought stress poses a significant challenge. By comparing different biochar amendment levels, we found that 5 tons per hectare was more effective than 10 tons per hectare, offering a practical guideline for future biochar application strategies. The scientific contributions of this work extend to the enhancement of soil properties, such as water retention, organic matter content, and nutrient availability, which are critical for sustainable crop production under climate stress. However, the study is limited by its short-term scope; further longer-term field experiments are required to assess the enduring impacts of biochar on soil health and crop yield. Future research should explore biochar's effects across different soil types and climates, focusing on its integration with other sustainable agricultural practices. Policy implications include encouraging the use of biochar in drought-prone regions to improve food security, soil fertility, and water management. Furthermore, this work advocates for the development of guidelines and incentives for farmers to adopt biochar, contributing to sustainable agricultural systems.

Data availability

The datasets generated during and/or analyzed during the current study are available from the corresponding author on reasonable request.

Received: 3 September 2024; Accepted: 10 October 2024
Published online: 23 October 2024

References

1. Kim, J. H., Sung, J. H., Shahid, S. & Chung, E. S. Future hydrological drought analysis considering agricultural water withdrawal under SSP scenarios. *Water Resour. Manag.* **36**, 2931 (2022).
2. Sajjad, M. M. et al. Impact of climate and land-use change on groundwater resources, study of Faisalabad district. *Pakistan Atmos.* **13**, 1097 (2022).
3. Lesk, C. & Anderson, W. Decadal variability modulates trends in concurrent heat and drought over global croplands. *Environ. Res. Lett.* **16**, 55024 (2021).
4. Vicente-Serrano, S. M. et al. Global drought trends and future projections. *Philos. Trans. R Soc. A.* **380**, 20210285 (2022).
5. Khan, N. et al. Prediction of droughts over Pakistan using machine learning algorithms. *Adv. Water Resour.* **139**, 103562 (2020).
6. Ahmad, S. et al. Impact of water insecurity amidst endemic and pandemic in Pakistan: Two tales unsolved. *Ann. Med. Surg.* **81**, 104350 (2022).
7. Wang, X. Managing land carrying capacity: Key to achieving sustainable production systems for food security. *Land*. **11**, 484 (2022).
8. Salman, S. A. et al. Changes in climatic water availability and crop water demand for Iraq region. *Sustainability*. **12**, 3437 (2020).
9. Lema, B. et al. Evaluation of soil physical properties of long-used cultivated lands as a deriving indicator of soil degradation, north Ethiopia. *Phys. Geogr.* **40**, 323–338 (2019).
10. Jahan, S., Iqbal, S., Rasul, F. & Jabeen, K. Efficacy of biochar as soil amendments for soybean (*Glycine max* L.) morphology, physiology, and yield regulation under drought. *Arab. J. Geosci.* **13**, 1–20 (2020).
11. Kloss, S. et al. Biochar application to temperate soils: Effects on soil fertility and crop growth under greenhouse conditions. *J. Plant. Nutr. Soil. Sci.* **177**, 3–15 (2014).
12. Jamaludin, N., Rashid, S. A. & Tan, T. Natural biomass as carbon sources for the synthesis of photoluminescent carbon dots. In *Synthesis, Technology and Applications of Carbon Nanomaterials.* 109–134 (Elsevier, 2019).
13. Głąb, T., Palmowska, J., Zaleski, T. & Gondek, K. Effect of biochar application on soil hydrological properties and physical quality of sandy soil. *Geoderma*. **281**, 11–20 (2016).
14. Obia, A., Mulder, J., Martinsen, V., Cornelissen, G. & Børresen, T. In situ effects of biochar on aggregation, water retention and porosity in light-textured tropical soils. *Soil. Tillage Res.* **155**, 35–44 (2016).
15. Fischer, D. & Glaser, B. Synergisms between compost and biochar for sustainable soil amelioration. *Manag Org. Waste*. **1**, 167–198 (2012).
16. Abel, S. et al. Impact of biochar and hydrochar addition on water retention and water repellency of sandy soil. *Geoderma*. **202**, 183–191 (2013).
17. Abrol, V. et al. Biochar effects on soil water infiltration and erosion under seal formation conditions: Rainfall simulation experiment. *J. Soils Sediments*. **16**, 2709–2719 (2016).
18. Liu, N. et al. Role and multi-scale characterization of bamboo biochar during poultry manure aerobic composting. *Bioresour Technol.* **241**, 190–199 (2017).
19. Qambrani, N. A. et al. Biochar properties and eco-friendly applications for climate change mitigation, waste management, and wastewater treatment: A review. *Renew. Sustain. Energy Rev.* **79**, 255–273 (2017).
20. Razzaghi, F., Obour, P. B. & Arthur, E. Does biochar improve soil water retention? A systematic review and meta-analysis. *Geoderma*. **361**, 114055 (2020).
21. Dai, Z. et al. Association of biochar properties with changes in soil bacterial, fungal and fauna communities and nutrient cycling processes. *Biochar*. **3**, 239–254 (2021).
22. Chen, J., Lærke, P. E. & Jørgensen, U. Land conversion from annual to perennial crops: A win-win strategy for biomass yield and soil organic carbon and total nitrogen sequestration. *Agric. Ecosyst. Environ.* **330**, 107907 (2022).
23. Marsh, H. & Reinoso, F. R. Activated Carbon. 383–388. Elsevier, (2006).
24. Sajjadi, B., Chen, W. Y. & Egiebor, N. O. A comprehensive review on physical activation of biochar for energy and environmental applications. *Rev. Chem. Eng.* **35**, 735–776 (2019).

25. Usman, A. R. et al. Chemically modified biochar produced from conocarpus waste increases NO3 removal from aqueous solutions. *Environ. Geochem. Health*. **38**, 511–521 (2016).
26. Yuvaraj, A. et al. Activation of biochar through exoenzymes prompted by earthworms for vermibiochar production: A viable resource recovery option for heavy metal contaminated soils and water. *Chemosphere*. **278**, 130458 (2021).
27. Sanchez-Hernandez, J. C., Ro, K. S. & Díaz, F. J. Biochar and earthworms working in tandem: Research opportunities for soil bioremediation. *Sci. Total Environ*. **688**, 574–583 (2019).
28. Angın, D., Altintig, E. & Köse, T. E. Influence of process parameters on the surface and chemical properties of activated carbon obtained from biochar by chemical activation. *Bioresour. Technol.* **148**, 542–549 (2013).
29. Huff, M. D. & Lee, J. W. Biochar-surface oxygenation with hydrogen peroxide. *J. Environ. Manag*. **165**, 17–21 (2016).
30. Acemioğlu, B. Removal of a reactive dye using NaOH-activated biochar prepared from peanut shell by pyrolysis process. *Int. J. Coal Prep Util.* **42**, 671–693 (2022).
31. Sanchez-Hernandez, J. C. et al. Earthworms increase the potential for enzymatic bio-activation of biochars made from co-pyrolyzing animal manures and plastic wastes. *J. Hazard. Mater.* **408**, 124405 (2021).
32. Jahan, S., Ahmad, F., Rasul, F., Amir, R. & Shahzad, S. Physicochemical analysis of vermicompost-perlite based activated biochar and its influence on wheat (*Triticum aestivum* L.) growth under water stress. *J. Soil. Sci. Plant. Nutr.* **23**, 3034–3050 (2023).
33. Huma, B., Hussain, M., Ning, C. & Yuesuo, Y. Human benefits from maize. *Sch. J. Appl. Sci. Res.* **2**, 4–7 (2019).
34. Pahalvi, H. N. et al. Chemical fertilizers and their impact on soil health. *Microbiota Biofertilizers*. **2**, 1–20 (2021).
35. Sharafatmandrad, M. & Mashizi, A. K. Temporal and spatial assessment of supply and demand of the water-yield ecosystem service for water scarcity management in arid to semi-arid ecosystems. *Water Resour. Manag.* **35**, 63–82 (2021).
36. Rayment, G. E. & Higginson, F. R. Australian Laboratory Handbook of Soil and Water Chemical Methods. (1992).
37. Estefan, G. Methods of soil, plant, and water analysis: A Manual for the West Asia and North Africa Region. (2013).
38. Van Genuchten, M. T. A closed-form equation for predicting the hydraulic conductivity of unsaturated soils. *Soil. Sci. Soc. Am. J.* **44**, 892–898 (1980).
39. Anlauf, R. Using the EXCEL solver function to estimate the van Genuchten parameters from measured pF/water content values. (2014).
40. Allen, R. G., Pereira, L. S., Raes, D. & Smith, M. Crop evapotranspiration-Guidelines for computing crop water requirements-FAO Irrigation and drainage paper 56, Vol. 300 (Fao, Rome, 1998).
41. Howell, T. A. & Evett, S. The Penman-Monteith Method. USDA-Agricultural Research Service. In: Conservation & Production Research Laboratory, 14, Washington, DC (2004).
42. Piccinni, G., Ko, J., Marek, T. & Howell, T. Determination of growth-stage-specific crop coefficients (KC) of maize and sorghum. *Agric. Water Manag*. **96**, 1698–1704 (2009).
43. Sivakumar, M. V. K. & Shaw, R. H. Relative evaluation of water stress indicators for soybeans. *Agron. J.* **70**, 619–623 (1978).
44. Schneider, C. A., Rasband, W. S. & Eliceiri, K. W. NIH image to ImageJ: 25 years of image analysis. *Nat. Methods*. **9**, 671–675 (2012).
45. Radford, P. J. Growth analysis formulae-their use and abuse. *Crop Sci.* **7**, 171–175 (1967).
46. Russelle, M. P., Wilhelm, W. W., Olson, R. A. & Power, J. F. Growth analysis based on degree days. *Crop Sci.* **24**, 28–32 (1984).
47. Premachandra, G. S., Saneoka, H. & Ogata, S. Cell membrane stability, an indicator of drought tolerance, as affected by applied nitrogen in soyabean. *J. Agric. Sci.* **115**, 63–66 (1990).
48. Sairam, R. K. Effect of moisture-stress on physiological activities of two contrasting wheat genotypes. *Ind. J. Exp. Biol*. **32**, 594–597 (1994).
49. Bradford, M. M. A rapid and sensitive method for the quantitation of microgram quantities of protein utilizing the principle of protein-dye binding. *Anal. Biochem.* **72**, 248–254 (1976).
50. Prochazkova, D., Sairam, R. K., Srivastava, G. C. & Singh, D. V. Oxidative stress and antioxidant activity as the basis of senescence in maize leaves. *Plant. Sci.* **161**, 765–771 (2001).
51. Beauchamp, C. & Fridovich, I. Superoxide dismutase: Improved assays and an assay applicable to acrylamide gels. *Anal. Biochem.* **44**, 276–287 (1971).
52. Vetter, J. L., Steinberg, M. P. & Nelson, A. I. Enzyme assay, quantitative determination of peroxidase in sweet corn. *J. Agric. Food Chem.* **6**, 39–41 (1958).
53. Gorin, N. & Heidema, F. T. Peroxidase activity in Golden Delicious apples as a possible parameter of ripening and senescence. *J. Agric. Food Chem.* **24**, 200–201 (1976).
54. Shabbir, A. et al. Apparent and real water productivity for cotton-wheat zone of Punjab, Pakistan. *Pak J. Agric. Sci.* **49**, 357–363 (2012).
55. Liang, M. et al. Applications of biochar and modified biochar in heavy metal contaminated soil: A descriptive review. *Sustainability*. **13**, 14041 (2021).
56. Saeed, U., Wajid, S. A., Khaliq, T. & Zahir, Z. A. Optimizing irrigation and nitrogen for wheat through empirical modeling under semi-arid environment. *Environ. Sci. Pollut Res.* **24**, 11663–11676 (2017).
57. Verheijen, F. G. et al. The influence of biochar particle size and concentration on bulk density and maximum water holding capacity of sandy vs sandy loam soil in a column experiment. *Geoderma*. **347**, 194–202 (2019).
58. Jahan, S. et al. Chitosan beads-infused biochar for enhancing physio-chemical and yield attributes of sunflower (*Helianthus annuus* L.) grown under wastewater irrigation. *J. Soil. Sci. Plant. Nutr.* **1**, 1–22 (2024).
59. Han, L. et al. Biochar's stability and effect on the content, composition and turnover of soil organic carbon. *Geoderma*. **364**, 114184 (2020).
60. Zhao, C. et al. Comparing the effects of biochar and straw amendment on soil carbon pools and bacterial community structure in degraded soil. *J. Soil. Sci. Plant. Nutr.* **20**, 751–760 (2020).
61. Hossain, M. Z. et al. Biochar and its importance on nutrient dynamics in soil and plant. *Biochar*. **2**, 379–420 (2020).
62. Alhani, I. J. et al. Mechanical response of saturated and unsaturated gravels of different sizes in drained triaxial testing. *Acta Geotech.* **15**, 3075–3093 (2020).
63. Al-Bared, M. A. M., Marto, A. & Latifi, N. Utilization of recycled tiles and tyres in stabilization of soils and production of construction materials–A state-of-the-art review. *KSCE J. Civil Eng.* **22**, 3860–3874 (2018).
64. Rijk, I. et al. Biochar and peat amendments affect nitrogen retention, microbial capacity and nitrogen cycling microbial communities in a metal and polycyclic aromatic hydrocarbon contaminated urban soil. *Sci. Total Environ.* **936**, 173454 (2024).
65. Jahan, S., Iqbal, S., Rasul, F. & Jabeen, K. Structural characterization of soil biochar amendments and their comparative performance under moisture deficit regimes. *Arab. J. Geosci.* **12**, 1–15 (2019).
66. Tanure, M. M. C. et al. Soil water retention, physiological characteristics, and growth of maize plants in response to biochar application to soil. *Soil. Tillage Res.* **192**, 164–173 (2019).
67. Alghamdi, A. G., Alkhasha, A. & Ibrahim, H. M. Effect of biochar particle size on water retention and availability in a sandy loam soil. *J. Saudi Chem. Soc.* **24**, 1042–1050 (2020).
68. Xiu, L. et al. Biochar can improve biological nitrogen fixation by altering the root growth strategy of soybean in Albic soil. *Sci. Total Environ.* **773**, 144564 (2021).
69. Chang, Y. et al. Biochar improves soil physical characteristics and strengthens root architecture in Muscadine grape (*Vitis rotundifolia* L. *Chem. Biol. Technol. Agric.* **8**, 1–11 (2021).

70. Song, X. et al. Combined biochar and nitrogen application stimulates enzyme activity and root plasticity. *Sci. Total Environ.* **735**, 139393 (2020).
71. Yan, T., Xue, J., Zhou, Z. & Wu, Y. Biochar-based fertilizer amendments improve the soil microbial community structure in a karst mountainous area. *Sci. Total Environ.* **794**, 148757 (2021).
72. Preetiva, B., Chaubey, A. K. & Singsit, J. S. Biochar-mediated nutrients and microbial community dynamics in montane landscapes. *Underst. Soils Mounta Landsc.* **10**, 165–181 (2023).
73. Zhang, C. et al. Insight into soil microbial mechanisms on soil restoration via biochar application: Core microbial communities and nutrient cycling. *Environ. Res.* **228**, 115895 (2023).
74. Kapoor, A., Sharma, R., Kumar, A. & Sepehya, S. Biochar as a means to improve soil fertility and crop productivity: A review. *J. Plant. Nutr.* **45**, 2380–2388 (2022).
75. Adhikari, S., Moon, E. & Timms, W. Identifying biochar production variables to maximize exchangeable cations and increase nutrient availability in soils. *J. Clean. Prod.* **446**, 141454 (2024).
76. Rizwan, M., Nawaz, A., Irshad, S. & Manoharadas, S. Exogenously applied melatonin enhanced chromium tolerance in pepper by up-regulating the photosynthetic apparatus and antioxidant machinery. *Scientia Hortic.* **323**, 112468 (2024).
77. Yan, S., Weng, B., Jing, L. & Bi, W. Effects of drought stress on water content and biomass distribution in summer maize (*Zea mays* L). *Front. Plant. Sci.* **14**, 1118131 (2023).
78. Wu, J. et al. Physiology of plant responses to water stress and related genes: A review. *Forests*. **13**, 324 (2022).
79. Kang, M. W. et al. Enhancement of soil physical properties and soil water retention with biochar-based soil amendments. *Sci. Total Environ.* **836**, 155746 (2022).
80. Antonangelo, J. A., Culman, S. & Zhang, H. Comparative analysis and prediction of cation exchange capacity via summation: Influence of biochar type and nutrient ratios. *Front. Soil. Sci.* **4**, 1371777 (2024).
81. Cen, R. et al. Effect mechanism of biochar application on soil structure and organic matter in semi-arid areas. *J. Environ. Manag.* **286**, 112198 (2021).
82. Huang, X. et al. Biochar nanoparticles induced distinct biological effects on freshwater algae via oxidative stress, membrane damage, and nutrient depletion. *ACS Sustain. Chem. Eng.* **9**(32), 10761–10770 (2021).
83. Mansoor, S. et al. Biochar as a tool for effective management of drought and heavy metal toxicity. *Chemosphere*. **271**, 129458 (2021).
84. Ibrahim, M. F. et al. Melatonin counteracts drought induced oxidative damage and stimulates growth, productivity, and fruit quality properties of tomato plants. *Plants*. **9**(10), 1276 (2020).
85. Haider, F. U. et al. Integrated application of thiourea and biochar improves maize growth, antioxidant activity, and reduces cadmium bioavailability in cadmium-contaminated soil. *Front. Plant. Sci.* **12**, 809322 (2022).
86. Zafar, F., Noreen, Z., Shah, A. A. & Usman, S. Co-application of humic acid, potassium dihydrogen phosphate, and melatonin to ameliorate the effects of drought stress on barley (*Hordeum vulgare* L). *J. Soil. Sci. Plant. Nutr.* **24**(1), 618–634 (2024).
87. Irshad, M. K. et al. Goethite-modified biochar ameliorates the growth of rice (*Oryza sativa* L.) plants by suppressing cd and As-induced oxidative stress in cd and as co-contaminated paddy soil. *Sci. Total Environ.* **717**, 137086 (2020).
88. Zhao, W. et al. Effects of water stress on photosynthesis, yield, and water use efficiency in winter wheat. *Water*. **12**(8), 2127 (2020).
89. Razi, K. & Muneer, S. Drought stress-induced physiological mechanisms, signaling pathways and molecular response of chloroplasts in common vegetable crops. *Crit. Rev. Biotechnol.* **41**(5), 669–691 (2021).
90. Liang, G., Liu, J., Zhang, J. & Guo, J. Effects of drought stress on photosynthetic and physiological parameters of tomato. *J. Am. Soc. Hortic. Sci.* **145**(1), 12–17 (2020).
91. Jahan, S., Iqbal, S., Rasul, F. & Jabeen, K. Evaluating the effects of biochar amendments on drought tolerance of soybean (*Glycine Max* L.) using relative growth indicators. *Pak J. Bot.* **54**(5), 1629–1641 (2022).
92. Abideen, Z. et al. Ameliorating effects of biochar on photosynthetic efficiency and antioxidant defence of *Phragmites karka* under drought stress. *Plant. Biol.* **22**(2), 259–266 (2020).
93. Obadi, A. et al. Effect of biochar application on morpho-physiological traits, yield, and water use efficiency of tomato crop under water quality and drought stress. *Plants*. **12**(12), 2355 (2023).
94. Abd El-Mageed, T. A. et al. Acidified biochar as a soil amendment to drought stressed (*Vicia faba* L.) plants: Influences on growth and productivity, nutrient status, and water use efficiency. *Agronomy*. **11**(7), 1290 (2021).
95. Yildirim, E., Ekinci, M. & Turan, M. Impact of biochar in mitigating the negative effect of drought stress on cabbage seedlings. *J. Soil. Sci. Plant. Nutr.* **21**(3), 2297–2309 (2021).
96. Ghassemi Golezani, K. & Mousavi, S. A. Improving physiological performance and grain yield of maize by salicylic acid treatment under drought stress. *J. Plant. Physiol. Breed.* **12**(2), 1–10 (2022).
97. Sun, Y., Wang, C., Chen, H. Y. & Ruan, H. Response of plants to water stress: A meta-analysis. *Front. Plant. Sci.* **11**, 978 (2020).
98. Aslam, M. R. et al. Lead-immobilization, transformation, and induced toxicity alleviation in sunflower using nanoscale Fe°/BC: Experimental insights with mechanistic validations. *J. Plant. Interact.* **17**(1), 812–823 (2022).
99. Saleem, K. et al. Biochar-mediated control of metabolites and other physiological responses in water-stressed *Leptocohloa Fusca*. *Metabolites*. **13**(4), 511 (2023).
100. Farooq, M. et al. Integration of seed priming and biochar application improves drought tolerance in cowpea. *J. Plant. Growth Regul.* **40**, 1972–1980 (2021).
101. Ning, D. et al. Silicon-mediated physiological and agronomic responses of maize to drought stress imposed at the vegetative and reproductive stages. *Agronomy*. **10**(8), 1136 (2020).
102. Cohen, I., Zandalinas, S. I., Huck, C., Fritschi, F. B. & Mittler, R. Meta-analysis of drought and heat stress combination impact on crop yield and yield components. *Physiol. Plant.* **171**(1), 66–76 (2021).
103. Lalarukh, I. et al. Integral effects of brassinosteroids and timber waste biochar enhance the drought tolerance capacity of wheat plant. *Sci. Rep.* **12**(1), 12842 (2022).
104. Goodarzian-Ghahfarokhii, M., Mansouri-Far, C., Saeidi, M. & Abdoli, M. Different physiological and biochemical responses in maize hybrids subjected to drought stress at vegetative and reproductive stages. *Acta Biol. Szeged.* **60**(1), 27–37 (2016).
105. Hassan, N. M., El-Bastawisy, Z. M., El-Sayed, A. K., Ebeed, H. T. & Alla, M. M. N. Roles of dehydrin genes in wheat tolerance to drought stress. *J. Adv. Res.* **6**(2), 179–188 (2015).
106. Anjum, S. A. et al. Drought induced changes in growth, osmolyte accumulation, and antioxidant metabolism of three maize hybrids. *Front. Plant. Sci.* **8**, 69 (2017).
107. U. R. Farooqi, Z. et al. Regulation of drought stress in plants. *Plant. Life under Chan Env*. **10**, 77–104 (2020).
108. Liu, Y. et al. Biochar alleviates apple replant disease by reducing the growth of *Fusarium oxysporum* and regulating microbial communities. *Hortic. Plant. J.* **10**(3), 657–671 (2024).
109. Goodarzian Ghahfarokhi, M. et al. Effects of drought stress and rewatering on antioxidant systems and relative water content in different growth stages of maize (*Zea mays* L.) hybrids. *Arch. Agron. Soil. Sci.* **61**(4), 493–506 (2015).
110. Liu, S. et al. Comparative transcriptomic analysis of contrasting hybrid cultivars reveals key drought-responsive genes and metabolic pathways regulating drought stress tolerance in maize at various stages. *PLoS ONE* **15**(10), e0240468 (2020).
111. Sampathkumar, T., Pandian, B. J., Rangaswamy, M. V., Manickasundaram, P. & Jeyakumar, P. Influence of deficit irrigation on growth, yield, and yield parameters of cotton–maize cropping sequence. *Agric. Water Manag.* **130**, 90–102 (2013).
112. Haider, G. et al. Biochar but not humic acid product amendment affected maize yields via improving plant-soil moisture relations. *Plant. Soil.* **395**, 141–157 (2015).

113. Gale, N. V. & Thomas, S. C. Dose-dependence of growth and ecophysiological responses of plants to biochar. *Sci. Total Environ.* **658**, 1344–1354 (2019).
114. Diatta, A. A., Fike, J. H., Battaglia, M. L., Galbraith, J. M. & Baig, M. B. Effects of biochar on soil fertility and crop productivity in arid regions: A review. *Arab. J. Geosci.* **13**, 1–17 (2020).
115. Xue, P. et al. Effects of biochar and straw application on the soil structure and water-holding and gas transport capacities in seasonally frozen soil areas. *J. Environ. Manag.* **301**, 113943 (2022).
116. Xia, M. et al. Effect of various potassium agents on product distributions and biochar carbon sequestration of biomass pyrolysis. *Energy*. **289**, 130012 (2024).
117. Yin, X. et al. Effects of biochar on runoff generation, soil and nutrient loss at the surface and underground on the soil-mantled karst slopes. *Sci. Total Environ.* **889**, 164081 (2023).

Acknowledgements
The authors would like to extend their sincere appreciation to the National Research Program for Universities (NRPU Project No. 20-16716), Higher Education Commission (HEC) of Pakistan, and Researchers Supporting Project Number (RSP2024R182) King Saud University, Riyadh, Saudi Arabia.

Author contributions
MBN; Experimentation and Methodology, SJ; Supervision and Validation, AR; writing-original draft preparation and Statistical analysis, AAS; Conceptualization, Data curation and Formal analysis, VR & MAE; Conceptualization and Investigation. All authors read and approved the final manuscript.

Funding
National Research Program for Universities (NRPU Project No. 20-16716), Higher Education Commission (HEC) of Pakistan. Researchers Supporting Project Number (RSP2024R182) King Saud University, Riyadh, Saudi Arabia.

Declarations

Consent for publication
Not applicable.

Competing interests
The authors declare no competing interests.

Ethical approval and consent to participate
We declare that the manuscript reporting studies do not involve any human participants, human data or human tissues. So, it is not applicable. Our experiment follows with the relevant institutional, national, and international guidelines and legislation.

Additional information
Correspondence and requests for materials should be addressed to S.J. or A.A.S.

Reprints and permissions information is available at www.nature.com/reprints.

Publisher's note Springer Nature remains neutral with regard to jurisdictional claims in published maps and institutional affiliations.

Open Access This article is licensed under a Creative Commons Attribution-NonCommercial-NoDerivatives 4.0 International License, which permits any non-commercial use, sharing, distribution and reproduction in any medium or format, as long as you give appropriate credit to the original author(s) and the source, provide a link to the Creative Commons licence, and indicate if you modified the licensed material. You do not have permission under this licence to share adapted material derived from this article or parts of it. The images or other third party material in this article are included in the article's Creative Commons licence, unless indicated otherwise in a credit line to the material. If material is not included in the article's Creative Commons licence and your intended use is not permitted by statutory regulation or exceeds the permitted use, you will need to obtain permission directly from the copyright holder. To view a copy of this licence, visit http://creativecommons.org/licenses/by-nc-nd/4.0/.

© The Author(s) 2024